IMPULSIVE DIFFERENTIAL EQUATION MODEL IN HIV-1 INHIBITION. ADVANCES IN DUAL INHIBITORS OF HIV-1 REVERSE TRANSCRIPTASE & INTEGRASE FOR THE PREVENTION OF HIV-1 REPLICATION

S Mondal, J F Peters, P Ghosh, A K Sarkar

▶ **To cite this version:**

S Mondal, J F Peters, P Ghosh, A K Sarkar. IMPULSIVE DIFFERENTIAL EQUATION MODEL IN HIV-1 INHIBITION. ADVANCES IN DUAL INHIBITORS OF HIV-1 REVERSE TRANSCRIPTASE & INTEGRASE FOR THE PREVENTION OF HIV-1 REPLICATION. 2022. hal-03865639

HAL Id: hal-03865639

https://hal.science/hal-03865639v1

Preprint submitted on 22 Nov 2022

HAL is a multi-disciplinary open access archive for the deposit and dissemination of scientific research documents, whether they are published or not. The documents may come from teaching and research institutions in France or abroad, or from public or private research centers.

L'archive ouverte pluridisciplinaire **HAL**, est destinée au dépôt et à la diffusion de documents scientifiques de niveau recherche, publiés ou non, émanant des établissements d'enseignement et de recherche français ou étrangers, des laboratoires publics ou privés.

IMPULSIVE DIFFERENTIAL EQUATION MODEL IN HIV-1 INHIBITION. ADVANCES IN DUAL INHIBITORS OF HIV-1 REVERSE TRANSCRIPTASE & INTEGRASE FOR THE PREVENTION OF HIV-1 REPLICATION

S. MONDAL, J.F. PETERS, P. GHOSH, AND A.K. SARKAR

Abstract. This paper introduces an impulsive differential equation framework for calculating an effective dosing regimen for applying the dual inhibitors of HIV-1 reverse transcriptase (RT) and integrase (IN). Reverse transcriptase (RT) and integrase (IN) are two pivotal enzymes in HIV-1 replication. RT converts the single-stranded viral RNA genome into double-stranded DNA and IN catalyses the integration of viral double-stranded DNA into host DNA. The most successful treatment strategy for HIV-1 infection is Highly Active Antiretroviral Therapy (HAART), a combination of integrase inhibitor or entry inhibitor with reverse transcriptase inhibitor and protease inhibitor. Although HAART could successfully suppress the HIV-1 viral load and prevent the progression of HIV-1 infection into AIDS, it has several drawbacks, namely, long-term side effects, emergence of drug resistance profiles, poor patient compliance and intolerable toxicities. Currently, dual inhibitors of HIV-1 RT and IN have become a hotspot in new anti-HIV drug research and development. A dual inhibitor of HIV-1 RT/IN does the same thing as the two independent drugs would do. In this article, we have studied the therapeutic benefit of dual inhibitor of HIV-1 RT/IN which simultaneously works as non-nucleoside reverse transcriptase inhibitor (NNRTI) and integease inhibitor. By using impulsive differential equations, we have determined a periodic dosing regimen for applying the dual inhibitor of HIV-1 RT/IN. Analytically we have shown the non-negativity, boundedness of the HIV-1 RT/IN catalysed reaction model and established the existence condition and local stability of the periodic solution at steady-state for the case of multiple dose administration of dual inhibitor of HIV-1 RT/IN to controlling the replication process. The results obtained from analytical as well as numerical study provide a basic idea to investigate the minimum dose with highest efficacy and to calculate an effective and safe dosing interval of dual inhibitors of HIV-1 RT/IN to beat the virus.

Contents

2010 *Mathematics Subject Classification.* 35R12 (Impulsive differential equations); 35B10 (Periodic solutions to differential equations).

Key words and phrases. AIDS, Dual Inhibitors,d HIV, Impulsive differential equation, Integrase, Reverse Transcriptase.

The research by J.F. Peters has been supported by the Natural Sciences & Engineering Research Council of Canada (NSERC) discovery grant 185986 and Instituto Nazionale di Alta Matematica (INdAM) Francesco Severi, Gruppo Nazionale per le Strutture Algebriche, Geometriche e Loro Applicazioni grant 9 920160 000362, n.prot U 2016/000036 and Scientific and Technological Research Council of Turkey (TÜBİTAK) Scientific Human Resources Development (BIDEB) under grant no: 2221-1059B211301223.

1. Introduction

Acquired immunodeficiency syndrome (AIDS) is a lethal disease caused by human immunodeficiency virus (HIV) infection. According to UNAIDS, at the end of 2020, around 37.7 million of people were lived with HIV, among them 1.7 million of people were newly infected [36]. Although no cure has yet been developed, the most effective treatment regimen for HIV-1 infection is Highly Active Antiretroviral Therapy (HAART), a combination of 3 or 4 anti-AIDS drugs [11]. HAART could successfully keep the viral load in a low level and evidently reduce the mortality of HIV-1 infected people, but it involves the difficulty of perfect adherence because of complicated dosing and intolerable toxicities. Recently, dual inhibitors of HIV-1 reverse transcriptase and integrase (Portmanteau Inhibitors) to facilitate patient compliance have become a promising scientific endeavour [8], [15].

The HIV-1 RT/IN dual inhibitors each of which is a single chemical entity capable of inhibiting both the enzymes reverse transcriptase (RT) and integrase (IN) is less likely to develop drug resistance from the virus because of its multi-faceted approach and cost effectiveness. Reverse Transcriptase Inhibitors fall into two categories: Nucleoside Reverse Transcriptase Inhibitors (NRTIs) and Non-Nucleoside Reverse Transcriptase Inhibitors (NNRTIs). NRTIs as competitive inhibitors act as chain terminators, whereas NNRTIs allosterically inhibit DNA polymerisation. NRTIs not only interfere with the replication of viral DNA and RNA, but also influence normal cell DNA replication due to its poor selectivity [12]. NNRTIs target the allosteric site of the viral Reverse Transcriptase (RT), change the conformation of the enzyme, interfere the binding between the enzyme bonds and substrate and inhibit in a non-competitive way [23], [25], [31]. Recently approved Integrase Inhibitors (raltegravir and elvitegravir) bind the active site of HIV-1 integrase in a pre-integration complex and block the viral DNA integration into host cell chromosomes [3], [30]. In this paper, we have used dual inhibitor of HIV-1 RT/IN taking bisheteroarylpiperazine compounds (Ex: Delavirdine, Atevirdine) as NNRTI and β-diketo acids (DKAs) group as integrase inhibitor. For better understanding the mechanisms of inhibition, it is important to have a clear view about the drug targets reverse transcriptase (RT) and integrase (IN) and the roles they play in the viral life cycle.

Viral infections are initiated by the interactions of the envelope glycoprotein with the CD4 receptor on the surface of immune cells and a co-receptor either CCR5 or CXCR4 that leads to a fusion of the membranes of the host cell and the virion [11], [16], [24]. This fusion introduces the viral core containing two copies of single-stranded viral RNA genome, about fifty copies of reverse Transcriptase (RT), integrase and other viral entities into the cytoplasm of the host cell [11], [16]. RT copies the single-stranded viral RNA genome into double-stranded DNA. This double-stranded DNA is carried into the nucleus of the infected cell and integrated to the host cell chromosome by another viral enzyme, integrase (IN) [16], [24]. RT has two catalytic domains: a DNA polymerase domain that can copy either an RNA or a DNA template and RNase H domain that cleaves RNA from an RNA-DNA hybrid [2], [16], [24]. Reverse transcription by the enzyme RT needs both a primer and a template as well as deoxyribonucleotide triphosphates (dNTPs). The viral RNA genome serves as the template and the primer for synthesis of the first DNA strand (minus strand) is a host tRNA [16], [24]. The RNA template forms a complex with the tRNA primer and the complex binds to the polymerase domain of the enzyme, followed by the addition of dNTPs. The dNTPs bind separately to another binding site of the polymerase domain and then catalytically added to the primer sequence [23]. Hence, RT starts to copy the 5' end of the viral RNA genome and generates an RNA-DNA hybrid [24]. As soon as the hybrid is made, RNase H domain degrades the 5' end of the RNA strand, making the newly synthesized minus-strand DNA single-stranded [16]. Now, RT starts to generate the second (plus) strand DNA by making a copy of the newly synthesized minus-strand DNA along with the first 18 nucleotides from the tRNA primer [16], [24]. As soon as tRNA has been copied into the DNA, RNase H domain of RT cleaves the tRNA primer and hence, finally double-stranded DNA is formed into the host cell cytoplasm [16], [18], [24]. Now this double-stranded DNA acts as a substrate for HIV-1 Integrase (IN). The integration process consists of two catalytic steps: 3' processing (3'-P) and strand transfer (ST). The processing reaction first takes place in the cytoplasm of infected cell. The enzyme removes two nucleotides from each 3' end of the viral DNA and forms IN-HIV DNA complex (pre integration complex) [13]. The pre integration complex is then transported into the nucleus of the host cell. Furthermore, the enzyme catalyses the insertion of the two processed 3' ends of viral DNA into opposite strands of the host DNA 5' phosphate ends by the reaction named as strand transfer and finally proviral DNA is formed [10]. In the final stage of viral life cycle, with the help of Protease enzyme, the viral assembly process is complete.

A handful of analytical works based on constructing dual inhibitors of HIV-1 RT/IN in the treatment of Acquired immunodeficiency syndrome (AIDS) have been performed and the efficacy of these HIV-1 RT/IN dual inhibitors in combating the HIV-1 infection have also been described theoretically [8], [15]. In 2007, Wang et al [33] designed dual inhibitors of HIV-1 RT and IN by merging a NNRTI such as 1-[(2-hydroxyethoxy) methyl]-6-(phenylthio) thymine (HEPT) and β-diketo acid derivatives (DKAs) as Integrase Inhibitors and showed that the merged compounds inhibited both the enzymes RT and IN at very low concentrations ($IC_{50RT} = 0.0092 - 0.23\mu M$, $IC_{50IN} = 1.8 - 7.7\mu M$). Next, in 2008, Wang and Vince [35] reported a new series of dual inhibitors of HIV-1 RT and IN by incorporating a diketo acid (DKA) fragment into the NNRTI delavirdine (for more details about

these dual inhibitors, see Appendix A). With the aim to enhance the anti-HIV efficacy, in 2015, He and Chen group [19] hybridized the NNRTI etravirine and integrase inhibitor GS-9137 to synthesize a new series of dual inhibitors of HIV-1 RT/IN. Despite having an ample number of theoretical works related to anti-HIV activities of these dual inhibitors, a mathematical model based analysis using HIV-1 RT/IN dual inhibitors is yet to be explored.

In the present paper, we consider a mathematical model on HIV-1 RT and IN catalysed reaction for HIV-1 replication with the understanding of Michaelis-Menten enzyme kinetic reaction. In the formulated model, we incorporate dual inhibitor of HIV-1 RT/IN which simultaneously works as a NNRTI and an integrase inhibitor. In order to determine an effective dosing regimen for applying the dual inhibitor of HIV-1 RT/IN, we use impulsive differential equations (IDEs) [17], [14] based on the steady-state Briggs-Haldane [5], [27] approximation for an enzyme kinetic reaction. Furthermore, by using Lambert W function [4], [29] we have obtained the analytical periodic solution for multiple dose administration and also established the expressions for maximum and minimum values of the periodic solution. Finally, we solve the model numerically and discuss the results from biological aspect. We hope these results may help the scientists to explore new treatment strategy in the fight against HIV-1 infection.

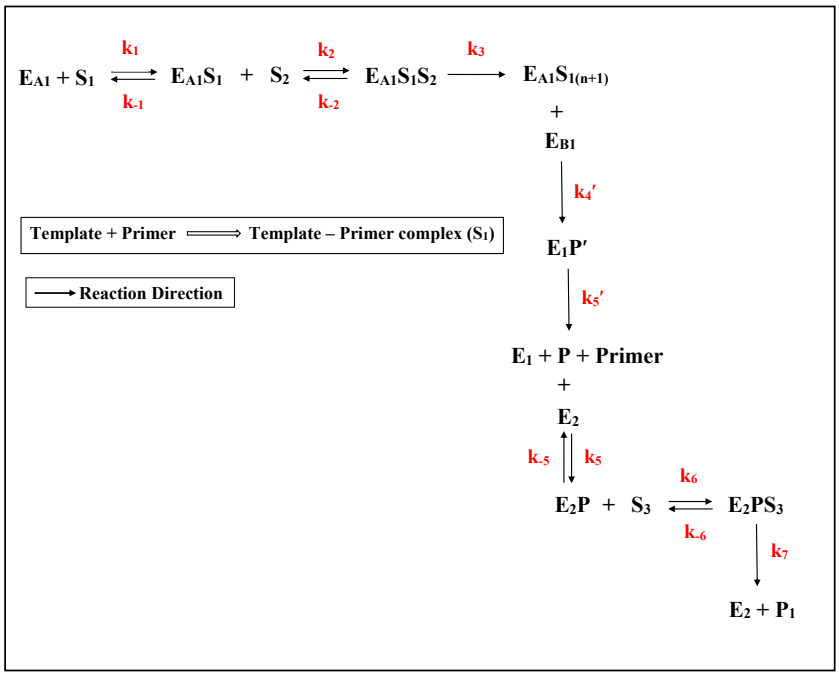

FIGURE 1. The schematic diagram of the enzymatic reactions.

2. PRELIMINARIES

Let E_1 denote the concentration of HIV-1 Reverse Transcriptase (RT), S_1 denote the concentration of viral single-stranded RNA template-primer complex and S_2

denote the concentration of deoxyribonucleotide triphosphate (dNTP). During Reverse transcription, the polymerase domain of Reverse Transcriptase (RT), i.e., E_{A1} starts to copy the viral RNA genome generating RT- RNA template-primer complex ($E_{A1}S_1$) and little portion of the complex reverts. For this reaction, the forward and backward rate constants are k_1 and k_{-1} respectively. The RT-RNA template-primer complex binds with dNTP (S_2) to yield RT-RNA template-primer-dNTP ($E_{A1}S_1S_2$) complex which finally formulates a new RT-RNA template - primer complex ($E_{A1}S_{1(n+1)}$). As DNA synthesis proceeds, the RNase H domain of Reverse Transcriptase (RT), i.e., E_{B1} binds with the complex $E_{A1}S_{1(n+1)}$ to produce linear single-stranded viral DNA (P) with $k_4{}'$ rate constant. And from this viral single-stranded DNA (P'), viral double-stranded DNA (P) is formed and the free RT (E_1) along with the primer gets released. The rate constant for this reaction is $k_5{}'$. Now the enzyme HIV-1 Integrase (E_2) combines with the newly formed double-stranded DNA (P) to yield Integrase-HIV DNA complex (E_2P). The Integrase-HIV DNA complex (E_2P) binds to the host DNA (S_3) inside the nucleus of the host cell and forms Integrase-HIV DNA-host DNA complex (E_2PS_3) that finally produces integrated proviral DNA (P_1) and releases free enzyme (E_2). The forward and backward rate constants for the integration process are $k_5, k_6, k_7, k_{-5}, k_{-6}$ respectively. The above facts are represented by the schematic diagram (1).
Since we mainly focus on polymerase chain reaction and integration process, we ignore the portion of RNase H mechanism from our model to reduce complexity during mathematical analysis. Therefore the revised schematic diagram (2) is presented below.

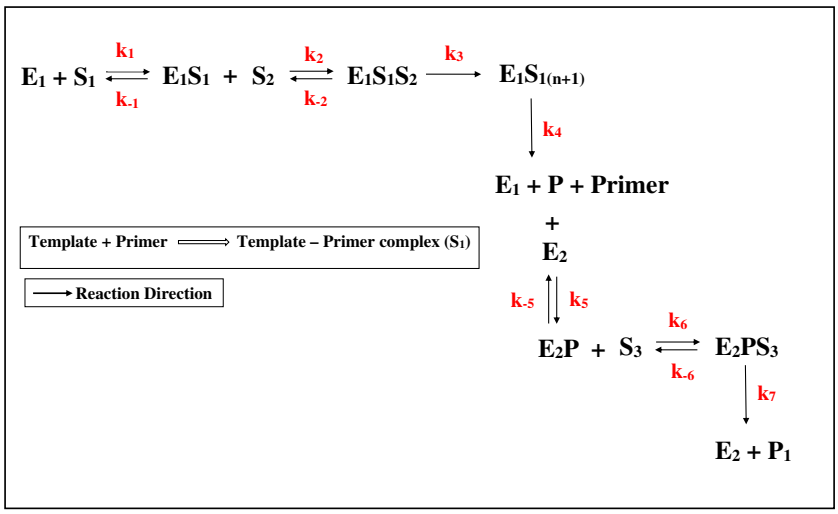

FIGURE 2. The revised schematic diagram of the enzymatic reactions.

Following the Law of Mass Action, the set of non-linear differential equations describing the above enzymatic reactions is as follows:

$$
\begin{aligned}
\frac{d[E_1]}{dt} &= -k_1[E_1][S_1] + k_{-1}[E_1S_1] + k_4[E_1S_{1(n+1)}],\\
\frac{d[S_1]}{dt} &= \lambda_1 - k_1[E_1][S_1] + k_{-1}[E_1S_1] - \mu_1[S_1],\\
\frac{d[S_2]}{dt} &= \lambda_2 - k_2[E_1S_1][S_2] + k_{-2}[E_1S_1S_2] - \mu_2[S_2],\\
\frac{d[E_1S_1]}{dt} &= k_1[E_1][S_1] - k_{-1}[E_1S_1] - k_2[E_1S_1][S_2] + k_{-2}[E_1S_1S_2],\\
\frac{d[E_1S_1S_2]}{dt} &= k_2[E_1S_1][S_2] - k_{-2}[E_1S_1S_2] - k_3[E_1S_1S_2],\\
\frac{d[E_1S_{1(n+1)}]}{dt} &= k_3[E_1S_1S_2] - k_4[E_1S_{1(n+1)}],\\
\frac{d[P]}{dt} &= k_4[E_1S_{1(n+1)}] - k_5[P][E_2] + k_{-5}[E_2P] - \mu_3P,\\
\frac{d[E_2]}{dt} &= -k_5[E_2][P] + k_{-5}[E_2P] + k_7[E_2PS_3],\\
\frac{d[E_2P]}{dt} &= k_5[E_2][P] - k_{-5}[E_2P] - k_6[E_2P][S_3] + k_{-6}[E_2PS_3],\\
\frac{d[S_3]}{dt} &= \lambda_3 - k_6[E_2P][S_3] + k_{-6}[E_2PS_3] - \mu_4[S_3],\\
\frac{d[E_2PS_3]}{dt} &= k_6[E_2P][S_3] - k_{-6}[E_2PS_3] - k_7[E_2PS_3],\\
\frac{d[P_1]}{dt} &= k_7[E_2PS_3] - \mu_5[P_1]. \qquad (1)
\end{aligned}
$$

where, λ_i is the external source rate of $S_i, i = \{1, 2, 3\}$ and μ_i is the natural decay rate of S_1, S_2, P, S_3 and P_1 respectively.

In order to simplify our model system, we use the steady-state Briggs-Haldane approximation [5], [27], i.e., shortly after initiation of the reaction, enzyme-substrate complex is formed at the same rate as it disappearances. Under this assumption, we get the following relations from system (1):

$$
\begin{aligned}
[E_1S_1] &= \frac{K_{M_{S_2}}[E_1][S_1]}{K_{S_1}K_{M_{S_2}} + K_{M_{S_1}}[S_2]},\\
[E_1S_1S_2] &= \frac{[E_1][S_1][S_2]}{K_{S_1}K_{M_{S_2}} + K_{M_{S_1}}[S_2]},\\
[E_1S_{1_{(n+1)}}] &= \frac{k_3[E_1][S_1][S_2]}{k_4(K_{S_1}K_{M_{S_2}} + K_{M_{S_1}}[S_2])},\\
[E_2P] &= \frac{K_{M_{S_3}}[E_2][P]}{K_PK_{M_{S_3}} + K_{M_P}[S_3]},\\
[E_2PS_3] &= \frac{[E_2][P][S_3]}{K_PK_{M_{S_3}} + K_{M_P}[S_3]}. \qquad (2)
\end{aligned}
$$

Substituting the expressions for $[E_1S_1], [E_1S_1S_2], [E_1S_{1_{(n+1)}}], [E_2P], [E_2PS_3]$ into (1) and using the relations $[E_1]_{10} = [E_1] + [E_1S_1] + [E_1S_1S_2] + [E_1S_{1_{(n+1)}}]$, $[E_2]_{20} =$

$[E_2] + [E_2P] + [E_2PS_3]$, we obtain the following five dimensional compartmental model:

$$
\begin{aligned}
\frac{d[S_1]}{dt} &= \lambda_1 - \frac{k_3[E]_{10}}{f([S_1],[S_2])}[S_1][S_2] - \mu_1[S_1],\\
\frac{d[S_2]}{dt} &= \lambda_2 - \frac{k_3[E]_{10}}{f([S_1],[S_2])}[S_1][S_2] - \mu_2[S_2],\\
\frac{d[P]}{dt} &= \frac{k_3[E]_{10}}{f([S_1],[S_2])}[S_1][S_2] - \frac{k_7[E]_{20}}{g([P],[S_3])}[P][S_3] - \mu_3[P],\\
\frac{d[S_3]}{dt} &= \lambda_3 - \frac{k_7[E]_{20}}{g([P],[S_3])}[P][S_3] - \mu_4[S_3],\\
\frac{d[P_1]}{dt} &= \frac{k_7[E]_{20}}{g([P],[S_3])}[P][S_3] - \mu_5[P_1]. \qquad (3)
\end{aligned}
$$

Where, $f([S_1],[S_2]) = K_{S_1}K_{M_{S_2}} + K_{M_{S_1}}[S_2] + K_{M_{S_2}}[S_1] + K_P{}'[S_1][S_2] + [S_1][S_2]$, $g([P],[S_3]) = K_PK_{M_{S_3}} + K_{M_P}[S_3] + K_{M_{S_3}}[P] + [P][S_3]$, $K_{S_1} = \frac{k_{-1}}{k_1}$, $K_{M_{S_1}} = \frac{k_3}{k_1}$, $K_{M_{S_2}} = \frac{k_{-2}+k_3}{k_2}$, $K_P{}' = \frac{k_3}{k_4}$, $K_P = \frac{k_{-5}}{k_5}$, $K_{M_P} = \frac{k_7}{k_5}$, $K_{M_{S_3}} = \frac{k_{-6}+k_7}{k_6}$ and $[E]_{i0}$ denotes the total concentration of the i^{th} enzyme, $i = \{1,2\}$. In this article, we have introduced the dual inhibitor of HIV-1 RT/IN (I) into the system. Here the drug (I) works as non-competitive and cooperatively binding inhibitor to bind E_1 and hence inactivates it by forming enzyme-inhibitor complex (E_1I). The forward and backward rate constants of this reaction are k_{i1} and k_{-i1} respectively. The E_1I complex could bind the substrate S_1 to yield a ternary complex E_1S_1I and the reaction dissociation constant between the complex E_1I and the substrate S_1 is $K_{S_1}{}'(= k_{-1}{}'/k_1{}')$. Alternatively, the inhibitor I can bind to the preformed E_1S_1 complex and thus E_1S_1I complex can also be generated with the rate constants $k_{i1}{}'$ and $k_{-i1}{}'$ respectively. In a similar manner, the $E_1S_1S_2I$ complex can be formed by binding of the E_1S_1I complex to the substrate S_2 or by binding of inhibitor I to the preordained $E_1S_1S_2$ complex, in either way. The forward and backward rate constants for these reactions are $k_2{}', k_{-2}{}'$ or $k_{i1}{}''$ and $k_{-i1}{}''$ respectively. The complex $E_1S_1S_2I$ then can go on to yield the complex $E_1S_{1_{(n+1)}}$ at a reduced rate compared to the uninhibited reaction. Besides acting as a non-competitive inhibitor toward E_1, the drug I simultaneously inhibits the enzyme (E_2) in an uncompetitive way by producing Integrase-HIV DNA-Inhibitor complex (E_2PI) and restrains the integration process. The forward and backward rate constants for this inhibition process are k_{i2} and k_{-i2} respectively. The entire system can be represented by the schematic diagram (3).

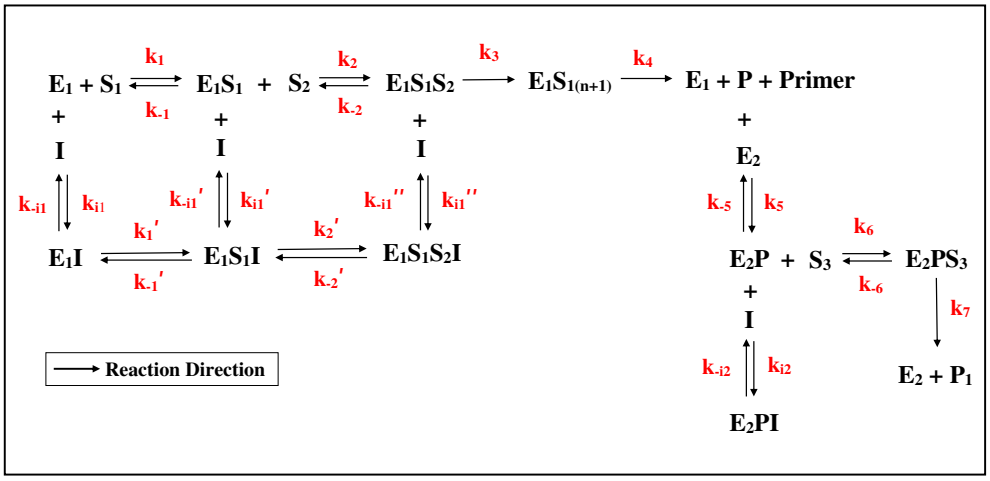

FIGURE 3. The schematic diagram of the enzymatic reactions.

Let, $[S_i] = S_i$, $i = \{1, 2, 3\}$, $[P] = P$, $[I] = I$ and $[E]_{j0} = E_{j0}$, $j = \{1, 2\}$. Using the steady state Briggs-Haldane kinetics, the model can be described as:

$$
\begin{aligned}
\frac{dS_1}{dt} &= \lambda_1 - \frac{k_3 E_{10}}{f_1(S_1, S_2, I)} S_1 S_2 - \mu_1 S_1, \\
\frac{dS_2}{dt} &= \lambda_2 - \frac{k_3 E_{10}}{f_1(S_1, S_2, I)} S_1 S_2 - \mu_2 S_2, \\
\frac{dP}{dt} &= \frac{k_3 E_{10}}{f_1(S_1, S_2, I)} S_1 S_2 - \frac{k_7 E_{20}}{g_1(P, S_3, I)} P S_3 - \mu_3 P, \\
\frac{dS_3}{dt} &= \lambda_3 - \frac{k_7 E_{20}}{g_1(P, S_3, I)} P S_3 - \mu_4 S_3, \\
\frac{dP_1}{dt} &= \frac{k_7 E_{20}}{g_1(P, S_3, I)} P S_3 - \mu_5 P_1, \\
\frac{dI}{dt} &= I_c - k_3 E_{10} [\frac{1}{h_1(I)} + \frac{1}{h_2(I)} + \frac{1}{h_3(I)}] I - \frac{k_7 E_{20}}{h_4(I)} I - \mu_6 I,
\end{aligned} \tag{4}
$$

with the initial concentrations $S_1(0) = S_{10}, S_2(0) = S_{20}, S_3(0) = S_{30}, P(0) = 0, P_1(0) = 0$, and $I(0) = I_0$. Here, $f_1(S_1, S_2, I) = (K_{S_1} K_{M_{S_2}} + K_{M_{S_1}} S_2) h_1(I) + K_{M_{S_2}} S_1 h_2(I) + S_1 S_2 h_3(I) + K_P{}' S_1 S_2$; $g_1(P, S_3, I) = K_P K_{M_{S_3}} + K_{M_P} S_3 + P S_3 + P K_{M_{S_3}} h_4(I)$; $h_1(I) = (1 + \frac{I^n}{K_{i1}{}^n})$, $h_2(I) = (1 + \frac{I^n}{(K_{i1}{}')^n})$, $h_3(I) = (1 + \frac{I^n}{(K_{i1}{}'')^n})$, $h_4(I) = (1 + \frac{I}{K_{i2}})$; n = Hill coefficient of inhibitor binding and the equilibrium dissociation constants K_{i1}, $K_{i1}{}'$, $K_{i1}{}''$, K_{i2} are given by the following:

$$
K_{i1} = \frac{k_{-i1}}{k_{i1}}, K_{i1}{}' = \frac{k_{-i1}{}'}{k_{i1}{}'}, K_{i1}{}'' = \frac{k_{-i1}{}''}{k_{i1}{}''}, K_{i2} = \frac{k_{-i2}}{k_{i2}}.
$$

3. MODEL PROPERTY

In this section, we have studied the non-negativity and boundedness of the reactants and stability of the interior equilibrium of system (4).

3.1. **Non-negativity and Boundedness.**

Theorem 1. *Each solution of the system (4) with initial conditions, remains non-negative for all $t \geqslant 0$ and uniformly bounded in the region Γ, where,*
$\Gamma = \{(S_1, S_2, P, S_3, P_1, I) \in \mathbb{R}^6_+ \mid 0 < S_1(t) \leq \frac{\lambda_1}{\mu_1}, 0 < S_2(t) \leq \frac{\lambda_2}{\mu_2}, 0 \leq P(t) \leq \frac{M_1}{\mu_3}, 0 \leq P_1(t) \leq \frac{M_2}{\mu_5}, 0 < I(t) \leq \frac{I_c}{\mu_6}\}$.

Proof. First, we show that $S_1(t)$ is positive for all $t \geqslant 0$. To see this, assume that t_0 be the first time when $S_1(t_0) = 0$. Now initially we have $S_1(t) > 0$ when $t = 0$. Therefore, $S_1(t) > 0$ for all $t \in [0, t_0)$. Substituting $t = t_0$ in the first equation of system (4), we get,

$$\begin{aligned} \frac{dS_1}{dt} &= \lambda_1 - \frac{k_3 E_{10} S_1(t_0) S_2(t_0)}{f_1(S_1(t_0), S_2(t_0), I(t_0)} - \mu_1 S_1(t_0) \\ &= \lambda_1 \\ &> 0. \end{aligned} \tag{5}$$

This means $S_1(t)$ is an increasing function at $t = t_0$. So, there exists an arbitrarily small $\epsilon > 0$ such that for all $t \in (t_0 - \epsilon, t_0) \subset [0, t_0)$, we have $S_1(t) < 0$. This is a contradiction to the fact that $S_1(t) > 0, \forall t \in [0, t_0)$. Hence, $S_1(t) > 0, \forall t \geqslant 0$.

Similarly, we can show that the components ($S_2(t), S_3(t), I(t)$ and $P(t)$) of our formulated model are positive for all $t \geqslant 0$. Again from the fifth equation of (4), we get

$$\begin{aligned} \frac{dP_1}{dt} &= \frac{k_7 E_{20}}{g_1(P, S_3, I)} P S_3 - \mu_5 P_1 \\ &> -\mu_5 P_1. \end{aligned} \tag{6}$$

But the initial value of P_1 is zero. So, we can write,

$$\frac{dP_1}{dt} \geqslant 0, \tag{7}$$

implies,

$$P_1 \geqslant 0. \tag{8}$$

Hence, we have the non-negativity of the solutions of the system (4) with the initial conditions.

Now we show that $S_1(t), S_2(t), P(t), S_3(t), P_1(t)$ and $I(t)$ are all bounded in their domains of definition. Taking first equation of (4), we get

$$\begin{aligned} \frac{dS_1}{dt} &= \lambda_1 - \frac{k_3 E_{10}}{f_1(S_1, S_2, I)} S_1 S_2 - \mu_1 S_1, \\ \Rightarrow \frac{dS_1}{dt} &\leqslant \lambda_1 - \mu_1 S_1 \end{aligned} \tag{9}$$

After integration, we have

$$S_1(t) \leqslant \frac{\lambda_1}{\mu_1}(1 - e^{-\mu_1 t}) + S_{10} e^{-\mu_1 t} \tag{10}$$

Thus, for sufficiently large t, we get the maximum value of template-primer complex presence in the case of HIV-1 infection as

$$\limsup_{t \to +\infty} S_1(t) \leqslant \frac{\lambda_1}{\mu_1} \tag{11}$$

Similarly, from second, fourth and sixth equations of (4), we can determine

$$\limsup_{t\to+\infty} S_2(t) \leqslant \frac{\lambda_2}{\mu_2}, \tag{12}$$

$$\limsup_{t\to+\infty} S_3(t) \leq \frac{\lambda_3}{\mu_4} \tag{13}$$

and

$$\limsup_{t\to+\infty} I(t) \leq \frac{I_c}{\mu_6} \tag{14}$$

Now considering the third equation of (4) we get the following inequality

$$\frac{dP}{dt} \leq \frac{k_3 E_{10} S_1 S_2}{f_1(S_1, S_2, I)} - \mu_3 P \tag{15}$$

Using the results obtained in (11), (12) and (14) one can get from the inequality (15),

$$\frac{dP}{dt} \leq M_1 - \mu_3 P \tag{16}$$

Solving the above inequality (16) for sufficiently large t, we get the following result,

$$\limsup_{t\to+\infty} P(t) \leq \frac{M_1}{\mu_3} \tag{17}$$

where,

$$M_1 = \frac{k_3 E_{10} \lambda_1 \lambda_2 {K_{i1}}^n ({K_{i1}}')^n ({K_{i1}}'')^n \mu_6^n}{\mu_1\beta_1\alpha_1 + K_{M_{S_2}}\lambda_1\mu_2\alpha_2 + \lambda_1\lambda_2\alpha_3 + {K_P}'\lambda_1\lambda_2\mu_6^n {K_{i1}}^n ({K_{i1}}')^n ({K_{i1}}'')^n}, \tag{18}$$

with $\beta_1 = (\mu_2 K_{S_1} K_{M_{S_2}} + K_{M_{S_1}}\lambda_2)$,$\alpha_1 = (I_c^n + {K_{i1}}^n\mu_6^n)({K_{i1}}')^n({K_{i1}}'')^n$, $\alpha_2 = (I_c^n + ({K_{i1}}')^n\mu_6^n){K_{i1}}^n({K_{i1}}'')^n$, $\alpha_3 = (I_c^n + ({K_{i1}}'')^n\mu_6^n){K_{i1}}^n({K_{i1}}')^n$.

From the fifth equation of system (4) and using the maximum values of P and S_3, the following inequality can be derived

$$\frac{dP_1}{dt} \leq M_2 - \mu_5 P_1. \tag{19}$$

In order to find the maximum value of Proviral DNA in HIV-1 infected patient, we solve the above inequality (19) for sufficiently large t and get,

$$\limsup_{t\to+\infty} P_1(t) \leq \frac{M_2}{\mu_5} \tag{20}$$

Where,

$$M_2 = \frac{k_7 E_{20} M_1 \lambda_3 \mu_6 K_{i2}}{\mu_3\mu_4\mu_6 K_P K_{M_{S_3}} + K_{M_P}\lambda_3\mu_3\mu_6 + M_1\lambda_3\mu_6 + M_1 K_{M_{S_3}}\mu_4(I_c + K_{i2})}. \tag{21}$$

Therefore all solutions of the system (4) are bounded. □

3.2. **Steady State Analysis.** The system (4) has at least one interior equilibrium, $E^*({S_1}^*, {S_2}^*, P^*, {S_3}^*, {P_1}^*, I^*)$, where ${S_1}^*, {S_2}^*, P^*, {S_3}^*, {P_1}^*$ and I^* are the positive roots of the following set of equations:

$$
\begin{aligned}
&\lambda_1 - \frac{k_3 E_{10}}{f_1({S_1}^*, {S_2}^*, I^*)} {S_1}^* {S_2}^* - \mu_1 {S_1}^* = 0,\\
&\lambda_2 - \frac{k_3 E_{10}}{f_1({S_1}^*, {S_2}^*, I^*)} {S_1}^* {S_2}^* - \mu_2 {S_2}^* = 0,\\
&\frac{k_3 E_{10}}{f_1({S_1}^*, {S_2}^*, I^*)} {S_1}^* {S_2}^* - \frac{k_7 E_{20}}{g_1(P^*, {S_3}^*, I^*)} P^* {S_3}^* - \mu_3 P^* = 0,\\
&\lambda_3 - \frac{k_7 E_{20}}{g_1(P^*, {S_3}^*, I^*)} P^* {S_3}^* - \mu_4 {S_3}^* = 0,\\
&\frac{k_7 E_{20}}{g_1(P^*, {S_3}^*, I^*)} P^* {S_3}^* - \mu_5 {P_1}^* = 0,\\
&I_c - k_3 E_{10}[\frac{1}{h_1(I^*)} + \frac{1}{h_2(I^*)} + \frac{1}{h_3(I^*)}]I^* - \frac{k_7 E_{20}}{h_4(I^*)} I^* - \mu_6 I^* = 0. \qquad (22)
\end{aligned}
$$

The Jacobin matrix J^* at the interior equilibrium point E^* is

$$
J^* = \begin{bmatrix}
-a_{11} - \mu_1 & -a_{12} & 0 & 0 & 0 & a_{16}\\
-a_{11} & -a_{12} - \mu_2 & 0 & 0 & 0 & a_{16}\\
a_{11} & a_{12} & -a_{33} - \mu_3 & -a_{34} & 0 & -a_{16} + a_{36}\\
0 & 0 & -a_{33} & -a_{34} - \mu_4 & 0 & a_{36}\\
0 & 0 & a_{33} & a_{34} & -\mu_5 & -a_{36}\\
0 & 0 & 0 & 0 & 0 & -a_{66} - \mu_6
\end{bmatrix}
$$

where,

$a_{11} = \frac{k_3 E_{10} h_1(I^*) {S_2}^* (K_{S_1} K_{M_{S_2}} + K_{M_{S_1}} {S_2}^*)}{(f_1({S_1}^*, {S_2}^*, I^*))^2}$, $a_{12} = \frac{k_3 E_{10} {S_1}^* K_{M_{S_2}} (K_{S_1} h_1(I^*) + {S_1}^* h_2(I^*))}{(f_1({S_1}^*, {S_2}^*, I^*))^2}$,

$a_{16} = \frac{k_3 E_{10} {S_1}^* {S_2}^* \{(K_{S_1} K_{M_{S_2}} + K_{M_{S_1}} {S_2}^*)({K_{i1}}')^n ({K_{i1}}'')^n + K_{M_{S_2}} {S_1}^* {K_{i1}}^n ({K_{i1}}'')^n + {S_1}^* {S_2}^* {K_{i1}}^n ({K_{i1}}')^n\} n {I^*}^{(n-1)}}{(f_1({S_1}^*, {S_2}^*, I^*))^2 {K_{i1}}^n ({K_{i1}}')^n ({K_{i1}}'')^n}$,

$a_{33} = \frac{k_7 E_{20} {S_3}^* (K_P K_{M_{S_3}} + K_{M_P} {S_3}^*)}{(g_1(P^*, {S_3}^*, I^*))^2}$, $a_{34} = \frac{k_7 E_{20} P^* (K_P K_{M_{S_3}} + K_{M_{S_3}} P^* h_4(I^*))}{(g_1(P^*, {S_3}^*, I^*))^2}$,

$a_{36} = \frac{k_7 E_{20} {P^*}^2 {S_3}^* K_{M_{S_3}}}{(g_1(P^*, {S_3}^*, I^*))^2 K_{i2}}$, $a_{66} = k_3 E_{10}[\frac{{K_{i1}}^n \{{K_{i1}}^n - (n-1){I^*}^n\}}{({K_{i1}}^n + {I^*}^n)^2} + \frac{({K_{i1}}')^n \{({K_{i1}}')^n - (n-1){I^*}^n\}}{\{({K_{i1}}')^n + {I^*}^n\}^2} + \frac{({K_{i1}}'')^n \{({K_{i1}}'')^n - (n-1){I^*}^n\}}{\{({K_{i1}}'')^n + {I^*}^n\}^2}] + \frac{k_7 E_{20} (K_{i2})^2}{\{K_{i2} + I^*\}^2}$.

Now the characteristic equation at the interior equilibrium point E^* is of the following form:

$$
(\mu_5 + x)(a_{66} + \mu_6 + x)\{x^2 + A_1 x + B_1\}\{x^2 + A_2 x 2 + B_2\} \quad = \quad 0. \qquad (23)
$$

where,
$A_1 = a_{33} + a_{34} + \mu_3 + \mu_4$, $B_1 = a_{33}\mu_4 + \mu_3(a_{34} + \mu_4)$, $A_2 = a_{11} + a_{12} + \mu_1 + \mu_2$,
$B_2 = a_{11}\mu_2 + \mu_1(a_{12} + \mu_2)$.
All the six eigenvalues are always negative. Therefore the interior equilibrium E^* is locally asymptotically stable.

4. Impulsive Model

The one-dimensional impulsive differential equation takes the form:

$$\begin{aligned} \frac{dI}{dt} &= -k_3E_{10}[\frac{1}{h_1(I)}+\frac{1}{h_2(I)}+\frac{1}{h_3(I)}]I-\frac{k_7E_{20}}{h_4(I)}I-\mu_6 I,\ for\ t\neq t_k, \\ & I(t_k^+)-I(t_k^-)=I_c\ for\ t=t_k. \end{aligned} \tag{24}$$

Where I is the concentration of the dual inhibitor of HIV-1 RT/IN with initial condition $I_0>0$. Here, I^+ and I^- are the concentrations of the inhibitor after and before impulse, respectively.
We calculate the rate equation of dual inhibitor of HIV-1 RT/IN in the following manner so that we can get some fruitful result from drug dynamics. The calculations are as follows:

$$\frac{dI}{dt} = -k_3E_{10}[\frac{1}{h_1(I)}+\frac{1}{h_2(I)}+\frac{1}{h_3(I)}]I-\frac{k_7E_{20}}{h_4(I)}I-\mu_6 I. \tag{25}$$

Where, $h_1(I)=(1+\frac{I^n}{{K_{i1}}^n})$, $h_2(I)=(1+\frac{I^n}{({K_{i1}}')^n})$, $h_3(I)=(1+\frac{I^n}{({K_{i1}}'')^n})$, $h_4(I)=(1+\frac{I}{K_{i2}})$; $n=$ Hill coefficient of inhibitor binding.

We see from above equation (25) that the dual inhibitor (I) of HIV-1 RT/IN exhibits simultaneous linear and nonlinear Michaelis-Menten elimination kinetics but the first-order elimination pathway is not that much important to determine the drug dose like the nonlinear Michaelis-Menten elimination pathway. So we can neglect the linear elimination part to avoid complexity in further calculations. Therefore, the rate equation of the inhibitor (I) takes the form:

$$\frac{dI}{dt} = -k_3E_{10}[\frac{1}{h_1(I)}+\frac{1}{h_2(I)}+\frac{1}{h_3(I)}]I-\frac{k_7E_{20}}{h_4(I)}I \tag{26}$$

Since the dual inhibitor (I) of HIV-1 RT/IN manifest two different parallel inhibition mechanisms, we divide the inhibitor (I) into two portions I_1 and I_2 in a way such that

$$\frac{dI}{dt} = \frac{dI_1}{dt}+\frac{dI_2}{dt} \tag{27}$$

where $I_1=\alpha I$ and $I_2=(1-\alpha)I$, $\alpha\in(0,1)$. Therefore, integrating the above Equation (27) and using the initial value conditions for $I(t)$, $I_1(t)$ and $I_2(t)$ we get

$$I(t) = I_1(t)+I_2(t) \tag{28}$$

Here I_1 working as a noncompetitive binding inhibitor shows intermolecular cooperativity to inhibit the enzyme RT (E_1) whereas I_2 uncompetitively inhibits the enzyme IN (E_2).
Hence, the rate equations for $I_1(t)$ and $I_2(t)$ are as follows:

$$\frac{dI_1}{dt} = -k_3E_{10}[\frac{1}{h_1(I_1)}+\frac{1}{h_2(I_1)}+\frac{1}{h_3(I_1)}]I_1 \tag{29}$$

and

$$\frac{dI_2}{dt} = -\frac{k_7E_{20}}{h_4(I_2)}I_2. \tag{30}$$

Here, $h_1(I_1)=(1+\frac{I_1^n}{{K_{i1}}^n})$, $h_2(I_1)=(1+\frac{{I_1}^n}{({K_{i1}}')^n})$, $h_3(I_1)=(1+\frac{{I_1}^n}{({K_{i1}}'')^n})$, $h_4(I_2)=(1+\frac{I_2}{K_{i2}})$; ${K_{i1}}'=\beta_1K_{i1}$ and ${K_{i1}}''=\beta_2K_{i1}$. ${K_{i1}}'\gtrless K_{i1}$ as well as ${K_{i1}}''\gtrless K_{i1}$

according to $\beta_1 \gtrless 1$ and $\beta_2 \gtrless 1$ respectively. In our case, we choose β_1, β_2 such that $1 < \beta_2 < \beta_1$.
Using the above mentioned relations between K_{i1}, ${K_{i1}}'$ and ${K_{i1}}''$, we can derive

$$\begin{aligned} h_1(I_1) &= 1 + \frac{I_1^n}{{K_{i1}}^n} \\ &> 1 + \frac{{I_1}^n}{({K_{i1}}')^n} \\ &= h_2(I_1) \end{aligned} \tag{31}$$

and

$$\begin{aligned} h_3(I_1) &= 1 + \frac{{I_1}^n}{({K_{i1}}'')^n} \\ &> 1 + \frac{{I_1}^n}{({K_{i1}}')^n} \\ &= h_2(I_1). \end{aligned} \tag{32}$$

Now replacing $h_1(I_1)$ and $h_3(I_1)$ by $h_2(I_1)$ in equation (29), we get the following inequality

$$\frac{dI_1}{dt} > \frac{-k_3 E_{10}}{h_2(I_1)} I_1$$

i.e.,

$$\frac{dI_1}{dt} > \frac{-k_3 E_{10} ({K_{i1}}')^n}{({K_{i1}}')^n + {I_1}^n} I_1. \tag{33}$$

We have derived the inequality (33) from the above calculation to determine the minimum permitted dose for the maximum toxicity, as the inhibitor (I) itself can be toxic for human body when presents in excess amount. So we have considered the equality with Equation (33) and formulated the impulsive differential equations for I_1 and I_2.
Hence, the impulsive differential equations for I_1 and I_2 take the form

$$\begin{aligned} \frac{dI_1}{dt} &= \frac{-k_3 E_{10} ({K_{i1}}')^n}{({K_{i1}}')^n + {I_1}^n} I_1, \ for\ t \neq t_k, \\ I_1(t_k^+) &- I_1(t_k^-) = \alpha I_c \ for\ t = t_k \end{aligned} \tag{34}$$

and

$$\begin{aligned} \frac{dI_2}{dt} &= \frac{-k_7 E_{20} K_{i2}}{K_{i2} + I_2} I_2, \ for\ t \neq t_k, \\ I_2(t_k^+) &- I_2(t_k^-) = (1-\alpha) I_c \ for\ t = t_k, \end{aligned} \tag{35}$$

where I_c is the fixed dose of dual inhibitor of HIV-1 RT/IN given on a fixed time interval τ. Here we consider the single impulse cycle $t_k \leq t \leq t_{k+1}$ such that $t_{k+1} - t_k = \tau$ and $k = 0, 1, 2, \cdots$. The general integrated form of the differential equations (34) and (35) are given by

$$\frac{1}{k_3 E_{10}} \left[ln \left(\frac{I_1(t_k^+)}{I_1(t)} \right) + \frac{1}{n({K_{i1}}')^n} \left(I_1(t_k^+)^n - I_1(t)^n \right) \right] = t - t_k \tag{36}$$

and

$$\frac{1}{k_7 E_{20}}\left[ln\left(\frac{I_2(t_k^+)}{I_2(t)}\right)+\frac{1}{K_{i2}}(I_2(t_k^+)-I_2(t))\right] = t-t_k. \tag{37}$$

However, to derive the exact closed form solutions for the differential Equations (34)-(35) [26], [29], we use the properties of the Lambert W function [9], [4], defined to be the multivalued inverse of the function $x \mapsto xe^x$ satisfying

$$LambertW(x)exp(LambertW(x)) = x. \tag{38}$$

Now Equations (36), (37) can be rewritten as:

$$ln\left(\frac{I_1(t)^n}{I_1(t_k^+)^n}\right)+\frac{I_1(t)^n}{({K_{i1}}')^n} = \frac{I_1(t_k^+)^n - n({K_{i1}}')^n k_3 E_{10}(t-t_k)}{({K_{i1}}')^n} \tag{39}$$

and

$$ln\left(\frac{I_2(t)}{I_2(t_k^+)}\right)+\frac{I_2(t)}{K_{i2}} = \frac{I_2(t_k^+) - K_{i2}k_7 E_{20}(t-t_k)}{K_{i2}},\ respectively. \tag{40}$$

Taking exponents of both sides on the above Equation (39) implies

$$\frac{I_1(t)^n}{({K_{i1}}')^n}exp\left(\frac{I_1(t)^n}{({K_{i1}}')^n}\right) = \frac{I_1(t_k^+)^n}{({K_{i1}}')^n}exp\left(\frac{I_1(t_k^+)^n - n({K_{i1}}')^n k_3 E_{10}(t-t_k)}{({K_{i1}}')^n}\right). \tag{41}$$

It follows from the definition of Lambert W function that we have the following explicit closed-form solution for model (34)

$$I_1(t)^n = ({K_{i1}}')^n LambertW\left(\frac{I_1(t_k^+)^n}{({K_{i1}}')^n}exp\left(\frac{I_1(t_k^+)^n - n({K_{i1}}')^n k_3 E_{10}(t-t_k)}{({K_{i1}}')^n}\right)\right). \tag{42}$$

Using similar approach, we derive the analytical solution for model (35) from Equation (40) as

$$I_2(t) = K_{i2}LambertW\left(\frac{I_2(t_k^+)}{K_{i2}}exp\left(\frac{I_2(t_k^+) - K_{i2}k_7 E_{20}(t-t_k)}{K_{i2}}\right)\right). \tag{43}$$

Actually, here $I_1(t)^n \equiv I_1(t)$ because $I_1(t)^n$ represents the total amount of the dual inhibitor (I) of HIV-1 RT/IN in the body at time t. Hence, denoting $I_1(t)^n$ by $I_1(t)$ in Equation (42) gives

$$I_1(t) = ({K_{i1}}')^n LambertW\left(\frac{I_1(t_k^+)}{({K_{i1}}')^n}exp\left(\frac{I_1(t_k^+) - n({K_{i1}}')^n k_3 E_{10}(t-t_k)}{({K_{i1}}')^n}\right)\right). \tag{44}$$

Therefore, the solution of model (24) at any interval $(t_k, t_{k+1}]$ is

$$\begin{aligned} I(t) &= I_1(t)+I_2(t) \\ \Rightarrow I(t) &= ({K_{i1}}')^n LambertW\left(\frac{I_1(t_k^+)}{({K_{i1}}')^n}exp\left(\frac{I_1(t_k^+) - n({K_{i1}}')^n k_3 E_{10}(t-t_k)}{({K_{i1}}')^n}\right)\right) \\ &+ K_{i2}LambertW\left(\frac{I_2(t_k^+)}{K_{i2}}exp\left(\frac{I_2(t_k^+) - K_{i2}k_7 E_{20}(t-t_k)}{K_{i2}}\right)\right). \end{aligned} \tag{45}$$

Now Equation (45) implies that

$$I(t_{k+1}^-) = I_1(t_{k+1}^-)+I_2(t_{k+1}^-)$$

Therefore,

$$\begin{aligned} I(t_{k+1}^{+}) &= I(t_{k+1}^{-}) + I_c \\ &= I_1(t_{k+1}^{-}) + I_2(t_{k+1}^{-}) + \alpha I_c + (1-\alpha) I_c \\ &= (I_1(t_{k+1}^{-}) + \alpha I_c) + (I_2(t_{k+1}^{-}) + (1-\alpha) I_c) \end{aligned}$$

$$\Rightarrow I(t_{k+1}^{+}) = I_1(t_{k+1}^{+}) + I_2(t_{k+1}^{+}). \tag{46}$$

We obtain the expressions for $I_1(t_{k+1}^{-})$, $I_2(t_{k+1}^{-})$ from Equations (44) and (43) respectively. Equation (44) implies that

$$I_1(t_{k+1}^{-}) = ({K_{i1}}')^n \, LambertW\left(\frac{I_1(t_k^{+})}{({K_{i1}}')^n} exp\left(\frac{I_1(t_k^{+}) - n({K_{i1}}')^n k_3 E_{10}(t_{k+1}-t_k)}{({K_{i1}}')^n}\right)\right) \tag{47}$$

This implies

$$\begin{aligned} I_1(t_{k+1}^{+}) &= I_1(t_{k+1}^{-}) + \alpha I_c \\ \Rightarrow I_1(t_{k+1}^{+}) &= ({K_{i1}}')^n \, LambertW\left(\frac{I_1(t_k^{+})}{({K_{i1}}')^n} exp\left(\frac{I_1(t_k^{+}) - n({K_{i1}}')^n k_3 E_{10}(t_{k+1}-t_k)}{({K_{i1}}')^n}\right)\right) + \alpha I_c. \end{aligned} \tag{48}$$

Similarly, considering equation (43) we can derive

$$I_2(t_{k+1}^{+}) = K_{i2} \, LambertW\left(\frac{I_2(t_k^{+})}{K_{i2}} exp\left(\frac{I_2(t_k^{+}) - K_{i2} k_7 E_{20}(t_{k+1}-t_k)}{K_{i2}}\right)\right) + (1-\alpha) I_c. \tag{49}$$

Now, equation (46) implies that there is positive periodic solution of model (24) if model (46) has atleast one positive steady-state. To find the steady-state concentration at any time t, we denote $I_k = I(t_{k+1}^{+})$, $I_{1_k} = I_1(t_{k+1}^{+})$, $I_{2_k} = I_2(t_{k+1}^{+})$. Then Equations (46) reduces to

$$I_k = I_{1_k} + I_{2_k} \tag{50}$$

where the expressions for I_{1_k} and I_{2_k} are represented by the following equations, substituting $t_{k+1} - t_k = \tau$

$$I_{1_k} = ({K_{i1}}')^n \, LambertW\left(\frac{I_{1_{k-1}}}{({K_{i1}}')^n} exp\left(\frac{I_{1_{k-1}} - n({K_{i1}}')^n k_3 E_{10}\tau}{({K_{i1}}')^n}\right)\right) + \alpha I_c \tag{51}$$

and

$$I_{2_k} = K_{i2} \, LambertW\left(\frac{I_{2_{k-1}}}{K_{i2}} exp\left(\frac{I_{2_{k-1}} - K_{i2} k_7 E_{20}\tau}{K_{i2}}\right)\right) + (1-\alpha) I_c. \tag{52}$$

Let k tend to infinity, the steady-state I^* satisfies the the following equation

$$I^* = I_1^* + I_2^*. \tag{53}$$

I_1^* and I_2^* are the respective steady-states of Equations (51)- (52) and satisfies

$$I_1^* = (K_{i1}')^n LambertW\left(\frac{I_1^*}{(K_{i1}')^n} exp\left(\frac{I_1^* - n(K_{i1}')^n k_3 E_{10}\tau}{(K_{i1}')^n}\right)\right) + \alpha I_c, \tag{54}$$

$$I_2^* = K_{i2} LambertW\left(\frac{I_2^*}{K_{i2}} exp\left(\frac{I_2^* - K_{i2} k_7 E_{20}\tau}{K_{i2}}\right)\right) + (1-\alpha) I_c. \tag{55}$$

Now Equation (54) implies that

$$\frac{I_1^* - \alpha I_c}{(K_{i1}')^n} = LambertW\left(\frac{I_1^*}{(K_{i1}')^n} exp\left(\frac{I_1^* - n(K_{i1}')^n k_3 E_{10}\tau}{(K_{i1}')^n}\right)\right). \tag{56}$$

It follows from the definition of Lambert W function that

$$\frac{I_1^* - \alpha I_c}{(K_{i1}')^n} exp\left(\frac{I_1^* - \alpha I_c}{(K_{i1}')^n}\right) = \frac{I_1^*}{(K_{i1}')^n} exp\left(\frac{I_1^* - n(K_{i1}')^n k_3 E_{10}\tau}{(K_{i1}')^n}\right) \tag{57}$$

which implies that there is a unique positive steady-state

$$I_1^* = \frac{\alpha I_c}{1 - exp\left(\frac{\alpha I_c - n(K_{i1}')^n k_3 E_{10}\tau}{(K_{i1}')^n}\right)} \tag{58}$$

provided

$$exp\left(\frac{\alpha I_c - n(K_{i1}')^n k_3 E_{10}\tau}{(K_{i1}')^n}\right) < 1.$$

Hence, we get the periodic solution of model (34) as

$$I_1(t) = (K_{i1}')^n LambertW\left(\frac{I_1^*}{(K_{i1}')^n} exp\left(\frac{I_1^* - n(K_{i1}')^n k_3 E_{10}(t-t_k)}{(K_{i1}')^n}\right)\right). \tag{59}$$

Similarly, we can show that the difference Equation (52) has a unique positive steady-state I_2^* and satisfies

$$I_2^* = \frac{(1-\alpha) I_c}{1 - exp\left(\frac{(1-\alpha) I_c - K_{i2} k_7 E_{20}\tau}{K_{i2}}\right)} \tag{60}$$

provided

$$exp\left(\frac{(1-\alpha) I_c - K_{i2} k_7 E_{20}\tau}{K_{i2}}\right) < 1$$

and thus the periodic solution of model (35) is

$$I_2(t) = K_{i2} LambertW\left(\frac{I_2^*}{K_{i2}} exp\left(\frac{I_2^* - K_{i2} k_7 E_{20}(t-t_k)}{K_{i2}}\right)\right). \tag{61}$$

Therefore, we can say that the difference Equation (50) has a unique positive steady-state I^* and verifies

$$I^* = \frac{\alpha I_c}{1 - exp\left(\frac{\alpha I_c - n({K_{i1}}')^n k_3 E_{10}\tau}{({K_{i1}}')^n}\right)} + \frac{(1-\alpha)I_c}{1 - exp\left(\frac{(1-\alpha)I_c - K_{i2}k_7E_{20}\tau}{K_{i2}}\right)} \tag{62}$$

if the following inequalities hold true:

$$\frac{\alpha I_c}{\tau} < n({K_{i1}}')^n k_3 E_{10} \tag{63}$$

and

$$\frac{(1-\alpha)I_c}{\tau} < K_{i2}k_7E_{20}. \tag{64}$$

Adding the above two inequalities (63) and (64), we obtain

$$\frac{I_c}{\tau} < n({K_{i1}}')^n k_3 E_{10} + K_{i2}k_7E_{20} \tag{65}$$

or

$$\tau > \frac{I_c}{n({K_{i1}}')^n k_3 E_{10} + K_{i2}k_7E_{20}} = \tau_{min}. \tag{66}$$

Thus the periodic solution of model (24) is given by

$$\begin{aligned} I(t) &= ({K_{i1}}')^n LambertW\left(\frac{I_1^*}{({K_{i1}}')^n} exp\left(\frac{I_1^* - n({K_{i1}}')^n k_3 E_{10}(t-t_k)}{({K_{i1}}')^n}\right)\right) \\ &+ K_{i2} LambertW\left(\frac{I_2^*}{K_{i2}} exp\left(\frac{I_2^* - K_{i2}k_7E_{20}(t-t_k)}{K_{i2}}\right)\right) \end{aligned} \tag{67}$$

where, the values of I_1^*, I_2^* are expressed by Equations (58), (60) respectively.
We see from the existence condition (65) that the model (24) has a unique periodic solution under the condition $\frac{I_c}{\tau} < (n({K_{i1}}')^n k_3 E_{10} + K_{i2}k_7E_{20})$. Moreover, we have shown the local stability of the periodic solution (67) (Appendix B). Obviously, Equation (62) implies that $I^* > I_c$. Hence, in order to design a periodic dosing regimen, one large initial dose I^* should be administered, following with a small dose I_c.
Let us denote the steady-state minimum and maximum concentrations as I_{min}^{ss} and I_{max}^{ss}, respectively. At the steady-state, these concentrations can be given by

$$\begin{aligned} I_{min}^{ss} &= ({K_{i1}}')^n LambertW\left(\frac{I_1^*}{({K_{i1}}')^n} exp\left(\frac{I_1^* - n({K_{i1}}')^n k_3 E_{10}\tau}{({K_{i1}}')^n}\right)\right) \\ &+ K_{i2} LambertW\left(\frac{I_2^*}{K_{i2}} exp\left(\frac{I_2^* - K_{i2}k_7E_{20}\tau}{K_{i2}}\right)\right) \end{aligned} \tag{68}$$

and

$$\begin{aligned} I_{max}^{ss} &= ({K_{i1}}')^n LambertW\left(\frac{I_1^*}{({K_{i1}}')^n} exp\left(\frac{I_1^* - n({K_{i1}}')^n k_3 E_{10}\tau}{({K_{i1}}')^n}\right)\right) \\ &+ K_{i2} LambertW\left(\frac{I_2^*}{K_{i2}} exp\left(\frac{I_2^* - K_{i2}k_7E_{20}\tau}{K_{i2}}\right)\right) + I_c \\ &\equiv I^*. \end{aligned} \tag{69}$$

5. Results and Discussion

To illustrate the behaviour of models, (3 and 4), we give numerical simulations with the set of parameter values in Table (1). Some of these values are estimated from [2], [8], [15], [21], [7], [1], [22], [20], [32], [37], [28], [6]. We begin by simulating the system without impulse, then with impulse.

Table 1. List of parameters

Parameter	Parameter description	Value (Unit)
k_3	The rate of the forward reaction from $E_1S_1S_2$ to $E_1S_{1_{n+1}}$	$(0.8-2.7)\ sec^{-1}$
k_7	The rate of the forward reaction from E_2PS_3 to E_2 and P_1	$(0.7-4.6)\ hr^{-1}$
K_{S_1}	Reaction dissociation constant between S_1 and E_1	$(0.0001-2.05)\ \mu M$
$K_{M_{S_1}}$	Michaelis constant for S_1	$(1.002-2.08)\ \mu M$
$K_{M_{S_2}}$	Michaelis constant for S_2	$(0.005-1.8)\ \mu M$
$K_{M_{S_3}}$	Michaelis constant for S_3	$(1.0-3.5)\ \mu M$
K_{M_P}	Michaelis constant for P	$(0.002-0.20)\ \mu M$
$K_P{}'$	Ratio of the forward rate constant from $E_1S_1S_2$ to $E_1S_{1_{n+1}}$ and from $E_1S_{1_{n+1}}$ to E_1+P	$(0.1-0.8)\ \mu M$
K_P	Reaction dissociation constant between P and E_2	$(0.02-1.03)\ \mu M$
K_{i1}	Reaction dissociation constant between E_1 and I	$(1.8-5.5)\ \mu M$
$K_{i1}{}'$	Reaction dissociation constant between E_1S_1 and I	$(10.0-15.0)\ \mu M$
$K_{i1}{}''$	Reaction dissociation constant between $E_1S_1S_2$ and I	$(5.7-10.0)\ \mu M$
K_{i2}	Reaction dissociation constant between E_2P and I	$(1.3-5.8)\ \mu M$
μ_1	Degradation rate of S_1	$(0.001-0.28)\ hr^{-1}$
μ_2	Degradation rate of S_2	$(0.02-0.5)\ hr^{-1}$
μ_3	Degradation rate of P	$(0.0001-0.4)\ hr^{-1}$
μ_4	Degradation rate of S_3	$(0.001-0.18)\ hr^{-1}$
μ_5	Degradation rate of P_1	$(0.02-0.3)\ hr^{-1}$

Figure (4), shows the reaction dynamics of formation of viral double-stranded DNA and integrated pro-viral DNA in HIV-1 infected patient. When an individual gets infected, a viral enzyme reverse transcriptase (RT) starts to synthesize double-stranded DNA ($P(t)$) from a viral single-stranded RNA genome with the help of deoxyribonucleotide triphosphates (dNTPs). The viral genome serving as an RNA template binds into a host tRNA primer and forms a template-primer complex ($S_1(t)$) that binds to one site on the enzyme. The dNTPs ($S_2(t)$) bind to another site on the enzyme and are then catalytically added to the primer sequence. The

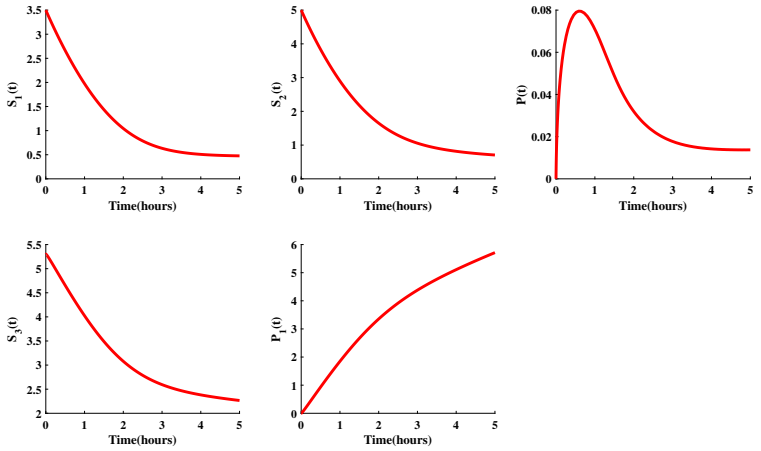

FIGURE 4. The nature of the curves of reactants in absence of HIV-1 RT/IN dual inhibitor, using $S_1(0) = 3.5\mu M$, $S_2(0) = 5\mu M$, $S_3(0) = 5.3\mu M$, $E_1(0) = 3\mu M$, $E_2(0) = 1.8\mu M$ as initial values. We have taken the parameter values from Table (1).

template-primer complex ($S_1(t)$) then starts to interact with the dNTPs ($S_2(t)$) and hence the synthesis process that is catalysed by enzyme RT of double-stranded DNA ($P(t)$) begins. So, the complex ($S_1(t)$) concentration and the dNTPs ($S_2(t)$) concentration decrease and the concentration of double-stranded DNA ($P(t)$) increases with time in a particular rate. Further, the double-stranded DNA ($P(t)$) is carried into the nucleus of the infected cell and it reacts with the host cell chromosome ($S_3(t)$) and these are converted into the final product integrated pro-viral DNA ($P_1(t)$) through the integration process catalysed by another viral enzyme integrase (IN). So, the concentration of viral double-stranded DNA ($P(t)$) and the host DNA ($S_3(t)$) concentration decrease while the integrated pro-viral DNA ($P_1(t)$) concentration increases. Here the first product double-stranded DNA ($P(t)$) which is generated from the template-primer-dNTPs reaction, acts as a substrate for the integration process. For being the product of one reaction and substrate of another, the concentration of viral double-stranded DNA ($P(t)$) first increases with time and then decreases. Except the concentrations of viral double-stranded DNA and integrated pro-viral DNA, we see similar nature of the curves of the components (S_1, S_2, S_3) participating in HIV-1 replication process.

Figure (5), describes the dynamics of formation of viral double-stranded DNA and integrated pro-viral DNA in HIV-1 infected patient after an immediate introduction of dual inhibitor of HIV-1 reverse transcriptase (RT) and integrase (IN) into the system. We have already mentioned that an RNA/DNA template-primer complex ($S_1(t)$) and the dNTPs ($S_2(t)$) interact with each other and these are converted into the first product viral double-stranded DNA ($P(t)$) in host cell cytoplasm through the process of reverse transcription catalysed by enzyme RT. So, the concentrations of the template-primer complex ($S_1(t)$) and the dNTPs ($S_2(t)$) decrease while the viral double-stranded DNA ($P(t)$) concentration increases. Furthermore, the double-stranded DNA ($P(t)$) is transported into the nucleus of the infected cell and

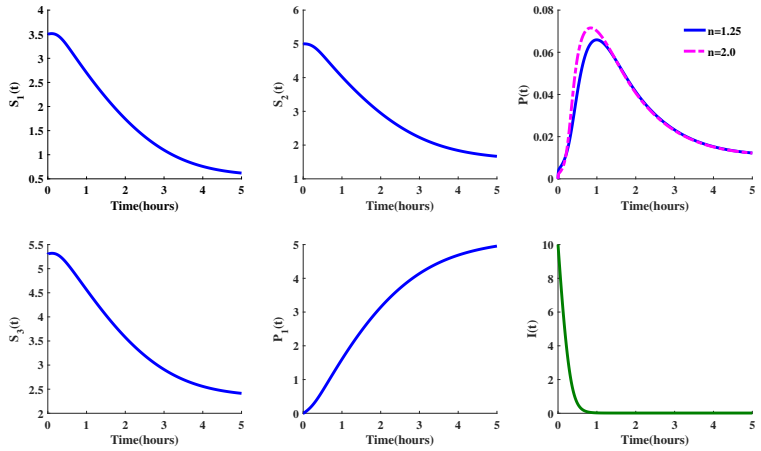

FIGURE 5. The nature of the curves of reactants in presence of HIV-1 RT/IN dual inhibitor with the initial conditions $S_1(0) = 3.5\mu M$, $S_2(0) = 5\mu M$, $S_3(0) = 5.3\mu M$, $E_1(0) = 3\mu M$, $E_2(0) = 1.8\mu M$, $I_0 = 10\mu M$. Here the parameter values are taken from Table (1).

transformed into the final product integrated pro-viral DNA ($P_1(t)$) after making an integration with the host cell chromosome ($S_3(t)$) by another viral enzyme, integrase (IN). Therefore the curve of double-stranded DNA ($P(t)$) concentration slows down like an uninhibited reaction when the concentration curve of integrated pro-viral DNA ($P_1(t)$) speeds up with time in a particular rate. Here we introduce the drug ($I(t)$) immediately after infection and the drug ($I(t)$) cooperatively (hill coefficient > 1) binds to enzyme RT and inactivates it in a non-competitive way, the curve defining the increasing rate of changes in double-stranded DNA ($P(t)$) concentration has a sigmoidal shape. Besides, the drug ($I(t)$) simultaneously works as an uncompetitive inhibitor towards enzyme IN and since no cooperativity (hill coefficient $= 1$) is shown for binding to enzyme IN, the concentration curve of integrated pro-viral DNA ($P_1(t)$) grows up in a hyperbolic nature. Also the curve that represents the host DNA ($S_3(t)$) concentration decreases in a similar way like the curves of S_1 and S_2. Hence, a detailed explanation is not necessary.

In Figure (6) we can see if we introduce dual inhibitor of HIV-1 reverse transcriptase and integrase in the system immediately, the formation of viral double-stranded DNA ($P(t)$) as well as integrated pro-viral DNA ($P_1(t)$) production slows down. Here we compare the reactants concentration in presence of dual inhibitor of HIV-1 RT/IN and in absence of dual inhibitor of HIV-1 RT/IN. Due to the non-competitive binding phenomena of the inhibitor ($I(t)$) towards enzyme RT, the progress curves of template-primer complex ($S_1(t)$) and the dNTPs ($S_2(t)$) go down at a reduced rate relative to the uninhibited reaction. A similar thing happens to the host DNA ($S_3(t)$) concentration curve as the drug simultaneously inhibits the enzyme IN in an uncompetitive way. The impact of the slower decrease of the reactants (S_1, S_2, S_3) is reflected on the formation of the other two components (P, P_1) participating in HIV-1 life cycle. We can see that in presence of the dual

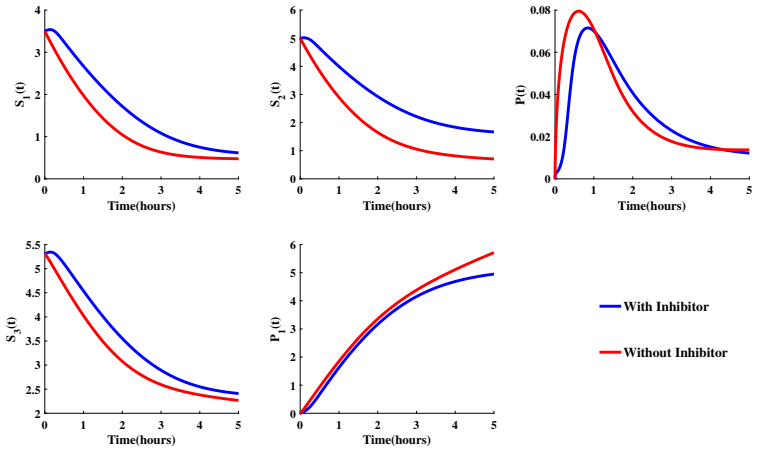

FIGURE 6. Comparison study between absence of HIV-1 RT/IN dual inhibitor and presence of HIV-1 RT/IN dual inhibitor for each reactant with initial conditions same as the above figures. Here also the parameter values are taken from Table (1).

inhibitor of HIV-1 RT/IN ($I(t)$), there is a sharp declination in the maximum velocity, i.e., in the peak point of double-stranded DNA ($P_1(t)$) progress curve. After achieving the maximum velocity, the double-stranded DNA ($P(t)$) concentration decreases with time at a lower rate comparing to the unrestrained reaction rate which is beneficial for an HIV-1 infected patient. Alternatively in presence of the dual inhibitor of HIV-1 RT/IN, the curve that represents the integrated pro-viral DNA ($P_1(t)$) concentration becomes lower than in absence of the inhibitor which is also very much advantageous for the patient. Integrated pro-viral DNA further takes part in the HIV-1 replication process, so the reduction of integrated pro-viral DNA concentration creates a favourable condition to suppressing the viral load in a low level. However, the effect of single dose of dual inhibitor of HIV-1 RT/IN on HIV-1 replication has been shown in Fig.(6) and we can see the benefits of using it for an HIV-1 infected individual introducing only once at intermediate stages of viral life cycle.

From Figure (7) we can get an overview of how fast the substrate template-primer complex (S_1) disappearances in the reaction pathway as well as how fast the substrate viral double-stranded DNA (P) is turned into the product integrated proviral DNA (P_1). The rate of disappearance of the substrate S_1 starts in a hyperbolic way because the velocity decreases proportionately with the substrate concentration. However, with further increases in substrate (S_1) concentration, the rate of decrease in the velocity slows down until a plateau is reached as the enzyme reverse transcriptase (E_1) becomes saturated. The reaction rate then decreases with increasing substrate (S_1) concentration, but most asymptotically approach the saturation rate. It is worth noting that in presence of the dual inhibitor of HIV-1 reverse transcriptase (RT) and integrase (IN), the rate of disappearances of substrate S_1 occurs in a slower motion than in absence of the inhibitor (I) because of non-competitive binding property of the inhibitor (I) towards enzyme RT (E_1)

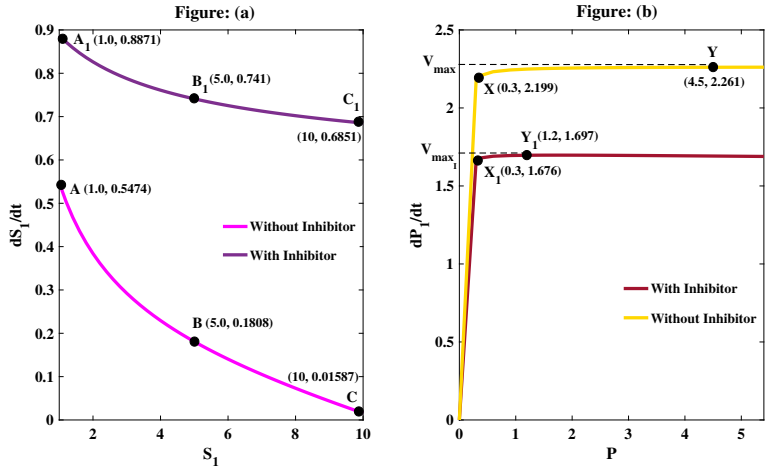

FIGURE 7. Comparison study between the plot of initial velocity as a function of substrate concentration in the presence of HIV-1 RT/IN dual inhibitor and in absence of HIV-1 RT/IN dual inhibitor and the parameter values are collected from Table (1).

and as a result, the saturation point $C_1(10, 0.8879)$ exists at a considerably upper position than the saturation point in absence of the dual inhibitor of HIV-1 RT/IN (I). In Figure $(7(b))$ we see an exact opposite nature between the positions of the saturation points from Figure $(7(a))$. Here as the substrate (P) concentration increases, so does the rate of reaction upto a certain point; at this point an optimal velocity (V_{max}) is reached. A continued increase in substrate (P) concentration produces no significant change in the reaction rate as there are not enough enzyme integrase (E_2) molecules available to break down the excess substrate (P) molecules. Since the dual inhibitor of HIV-1 RT/IN (I) simultaneously binds the enzyme integrase (E_2) in an uncompetitive way, the saturation point $Y_1(1.2, 1.697)$ exists at a lower position than the point $Y(3, 2.261)$ in absence of the dual inhibitor of HIV-1 RT/IN (I). Another noticeable feature of figure $(7(b))$ is that unlike figure $(7(a))$, the rate of reaction does not grow in a hyperbolic manner. Instead, the initial velocity tracks linearly with substrate (P) concentration as the enzyme (E_2) concentration is fixed at a higher value than the substrate (P) concentration and the concentration of substrate (P) is then titrated. However, from both the figures (fig.$7(a)$ & fig.$7(b)$), we are getting quite feasible and satisfactory results about the dual inhibitor of HIV-1 reverse transcriptase (RT) and integrase (IN) to control the HIV-1 infection.

We can notice as displayed in Figure (8) that I^{ss}_{min} and I^{ss}_{max} increase in a nonlinear way with respect to dose. However, for a fixed dose these concentrations are decreasing with respect to dosing interval τ. Here, we have taken period of dosing τ as 6h, 8h and observed the nature of the curves of I^{ss}_{min} and I^{ss}_{max}. Now, Eqns. (68, 69) clarify that I^{ss}_{min} or I^{ss}_{max} depends on the steady-state I^*. In combination with the existence condition (65), Figure (8) also describes that for given dose interval τ, the small dose I_c results in a small steady state I^* as well as a small maximum value of the periodic solution (67). This means that any solution of model (24)

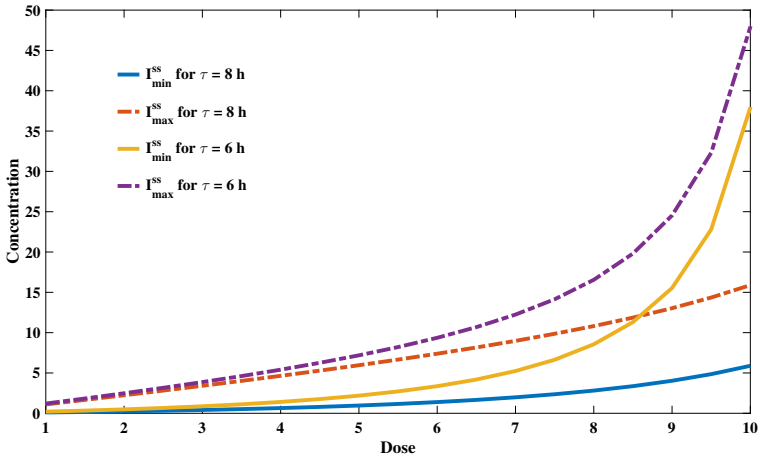

FIGURE 8. The relationships among the steady state, dose interval τ and dose I_c. Here we have taken $E_1(0) = 3\mu M$, $E_2(0) = 1.8\mu M$ and the parameter values are collected from Table(1).

approaches the periodic solution (67) at a higher speed in response to a smaller dose I_c. Figure (8) also confirms that the longer the dose interval is, the larger the dose can be used.

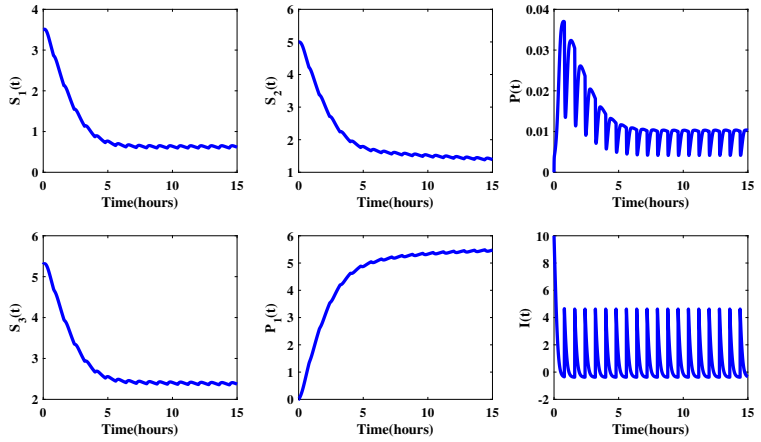

FIGURE 9. Concentration-time curves of the components of model (4) for the impulsive dosing of dual inhibitor of HIV-1 RT/IN with the initial conditions $S_1(0) = 3.5\mu M$, $S_2(0) = 5\mu M$, $S_3(0) = 5.3\mu M$, $E_1(0) = 3\mu M$, $E_2(0) = 1.8\mu M$, $I_0 = 10\mu M$, impulse dose input $I_c = 5\mu M$ and the time interval of dosing $\tau = 8h$. We have taken the parameter values from Table (1).

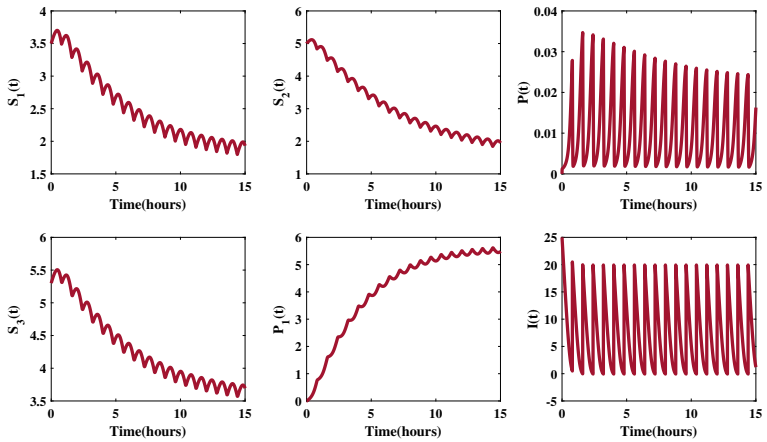

FIGURE 10. Concentration-time curves of all the reactants of model (4) for the impulsive dosing of HIV-1 RT/IN dual inhibitor with the initial conditions same as Fig. (9) except $I_0 = 25\mu M$, impulse dose input $I_c = 20\mu M$ and the time interval of dosing $\tau = 8h$. Here the parameter values are collected from Table (1).

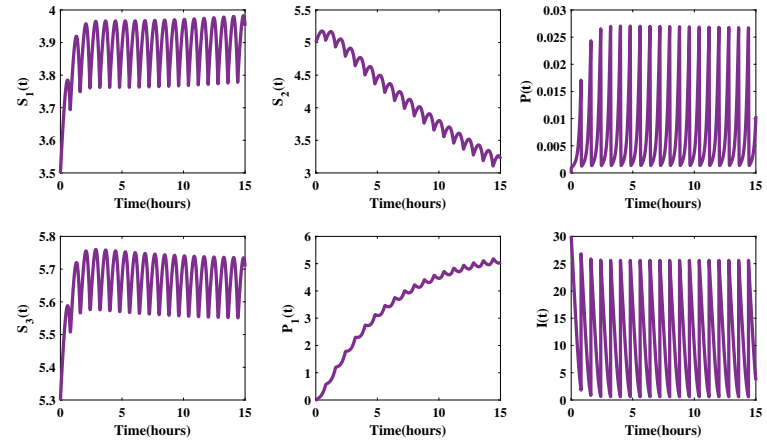

FIGURE 11. Curves of the components of model (4) for the impulsive dosing of dual inhibitor of HIV-1 RT/IN using the initial value $I_0 = 30\mu M$, impulse dose input $I_c = 25\mu M$ and the dosing interval $\tau = 8h$. The other initial and parameter values are fixed as those in Fig. (9).

Figures (9-13) represent the pattern of the curves of the components (viral single-stranded RNA (S_1), dNTPs (S_2), viral double-stranded DNA (P), host DNA (S_3), integrated proviral DNA (P_1), dual inhibitor (I) of HIV-1 reverse transcriptase and

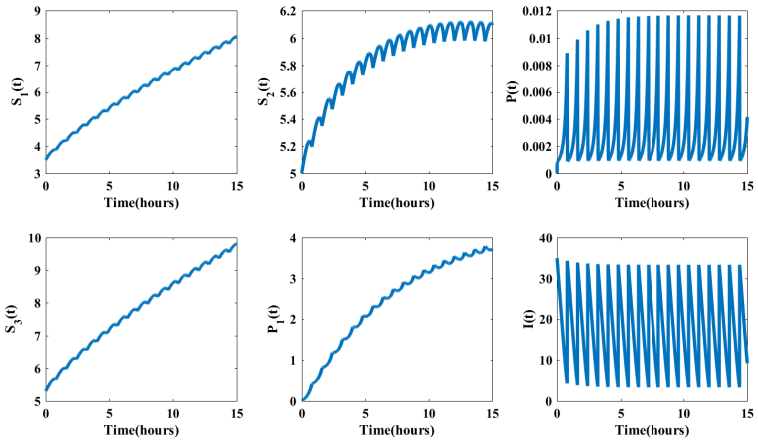

FIGURE 12. Nature of the curves of the components of model (4) for the impulsive dosing of dual inhibitor of HIV-1 RT/IN. Here the initial and parameter values are as like Fig. (9) except $I_0 = 35\mu M$, impulse dose input $I_c = 30\mu M$ and the period of dosing $\tau = 8h$.

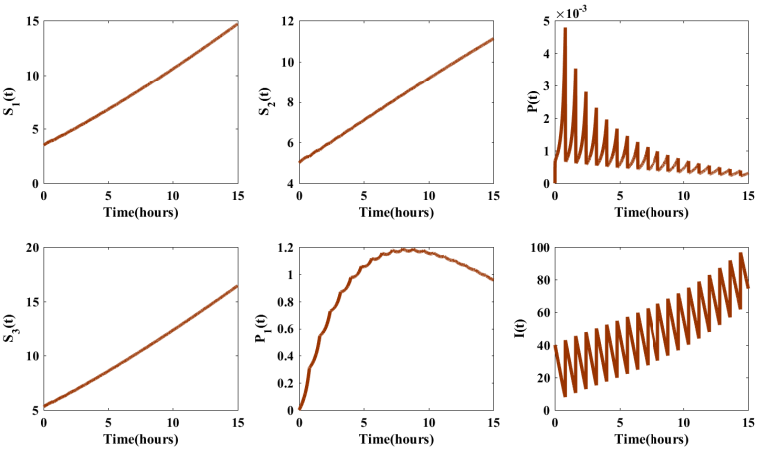

FIGURE 13. Curves of the components of model (4) for the impulsive dosing of dual inhibitor of HIV-1 RT/IN with the conditions $I_0 = 40\mu M$, impulse dose input $I_c = 35\mu M$ and the time interval of dosing $\tau = 8h$. The other initial values as well as the parameter values are same as Fig. (9).

integrase) involved in enzymatic reaction of dual inhibitor (I) of HIV-1 reverse transcriptase (RT) and integrase (IN). We apply the dual inhibitor (I) of HIV-1 RT/IN in intervals of 8 hour and vary the initial value ($I_0 = 10\mu M, 25\mu M, 30\mu M, 35\mu M, 40\mu M$ respectively) of the inhibitor (I) as well as the dose amount I_c ($= 5\mu M, 20\mu M, 25\mu M, 30\mu M, 35\mu M$) in each respective figure and observe the nature of the curves. Due to the impulsive

dosing of the dual inhibitor (I) of HIV-1 RT/IN, the fluctuating nature is seen in the curve of each component in all the figures except Fig. (13). In Figure (13), the fluctuating nature is negligible for the curves of the components $S_1(t)$, $S_2(t)$ and $S_3(t)$. We can notice as displayed in each figure from (9-13) that the concentration of viral double-stranded DNA (P) first increases then decreases and the process further continues whereas the inhibitor concentration (I) first decreases and then it increases, showing an exact opposite nature as compared to the curve of viral double-stranded DNA (P). It is worth noting that in Figure (9) the inhibitor concentration first reduces to zero but it does not rise up immediately, rather it becomes steady until the next dose is administered while in figure (10), the concentration of the inhibitor I immediately speeds up after being reduced to zero. The nature of the curves of other components $(S_1(t), S_2(t), S_3(t), P_1(t))$ in Figure (10) are quite similar as those of Figure (9) except the fact that the progress curves of $S_1(t)$, $S_2(t)$ and $S_3(t)$ in Figure (10) slow down at a reduced rate relative to those curves in Figure (9) whereas the growth curve of the integrated proviral DNA (P_1) in Figure (9) increases rapidly comparing to that curve in Figure (10). From Figure (11) the dual inhibitor (I) of HIV-1 RT/IN starts to dominate the viral replication process and as a result we see in Figure (11) that viral single-stranded RNA (S_1) concentration as well as the concentration of host DNA (S_3) increase while the concentration of dNTPs (S_2) decreases. In Figures (12-13), a complete dominating property of the inhibitor (I) to controlling the enzymatic reaction is seen and the reactants (S_1, S_2, P, S_3) do not get the scope to participate in the reaction mechanism. A noticeable feature in Figures (12-13) is that before the inhibitor (I) concentration could completely reduce to zero, the next dose is applied and hence, an immediate rise is seen in the inhibitor (I) concentration. Therefore, we can say that in Figure (9) the dose amount is not sufficient to controlling the viral replication whereas in Figure (11) the inhibitor (I) could reach the maximum therapeutic level and in Figures (12-13) it could exceed the maximum tolerance level of human body.

In Figures (14-18), we fix the initial value of the dual inhibitor (I) of HIV-1 RT/IN to $18\mu M$ as well as the constant dose I_c to $15\mu M$ and vary the dosing interval τ (=3h, 4h, 5h, 6h, 8h respectively). It is worth noting that the Figures (14-18) follow a reverse order in illustrating the nature of the curves of the components as Figures (9-13), i.e, the curves of the Figures (14-18) follow the nature of the curves of Figures (13-9) respectively. Hence, a detailed description is not needed here.

In Figure (19), we compare the viral double-stranded DNA (P) concentration as well as the integrated proviral DNA (P_1) concentration in absence of dual inhibitor (I) of HIV-1 RT/IN, in presence of dual inhibitor (I) of HIV-1 RT/IN with single dose and in presence of dual inhibitor (I) of HIV-1 RT/IN with multiple doses in impulsive way (taking the values same as Fig. (10) & Fig. (16)). In this figure we omit the curves of other components (viral single stranded RNA (S_1), dNTPs (S_2), host DNA (S_3), dual inhibitor (I) of HIV-1 RT/IN) to observe the changes of viral double-stranded DNA (P) concentration and integrated proviral DNA (P_1) concentration explicitly. We can see that the maximum velocity achieved by viral double-stranded DNA (P) in presence of the inhibitor (I) with a single dose is lower than the maximum velocity without inhibitor (I). Further, the declination in formation of viral double-stranded DNA (P) for multiple doses is very rapid as compared to the other two. The main reason for such a prominent decrease of viral

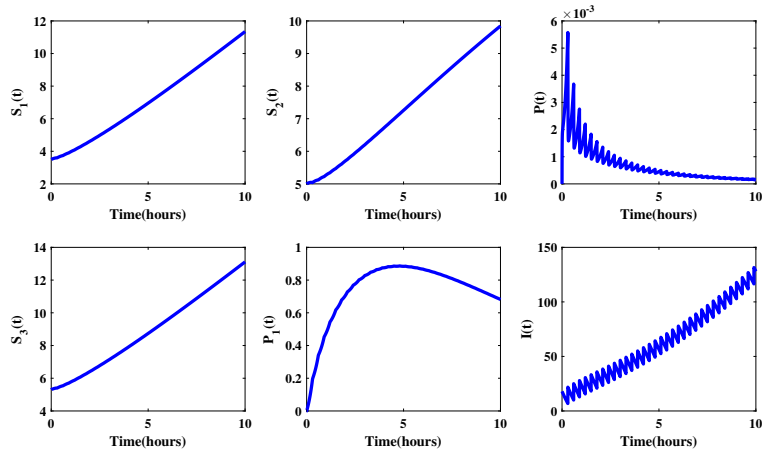

FIGURE 14. Concentration-time curves of the components of model (4) for the impulsive dosing of dual inhibitor of HIV-1 RT/IN with the initial conditions $S_1(0) = 3.5\mu M$, $S_2(0) = 5\mu M$, $S_3(0) = 5.3\mu M$, $E_1(0) = 3\mu M$, $E_2(0) = 1.8\mu M$, $I_0 = 18\mu M$, impulse dose input $I_c = 15\mu M$ and the time interval of dosing $\tau = 3h$. We have taken the parameter values from Table (1).

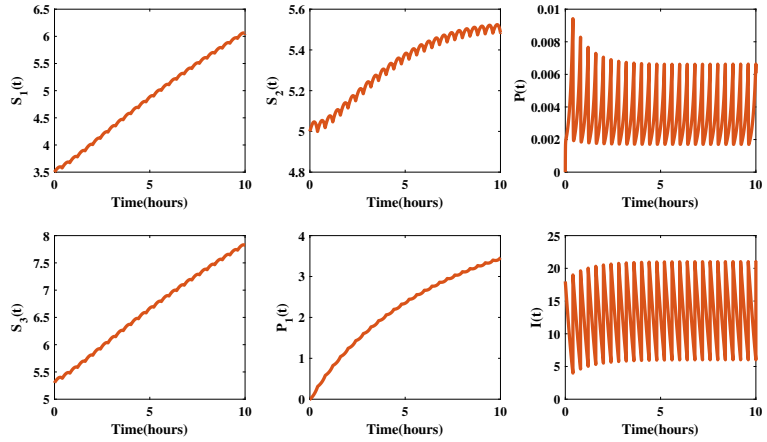

FIGURE 15. Curves of all the components of model (4) for the impulsive dosing of HIV-1 RT/IN dual inhibitor with the initial values and dose I_c same as Fig. (14). Here the dosing interval $\tau = 4h$ and the parameter values are taken from Table (1).

double-stranded (P) concentration is the inhibitory effect of the dual inhibitor (I) of HIV-1 RT/IN to combating the HIV-1 infection. A similar thing happens for the curves which represent the integrated proviral DNA (P_1) concentration. Here, we take two different impulse doses of the dual inhibitor (I) of HIV-1 RT/IN as

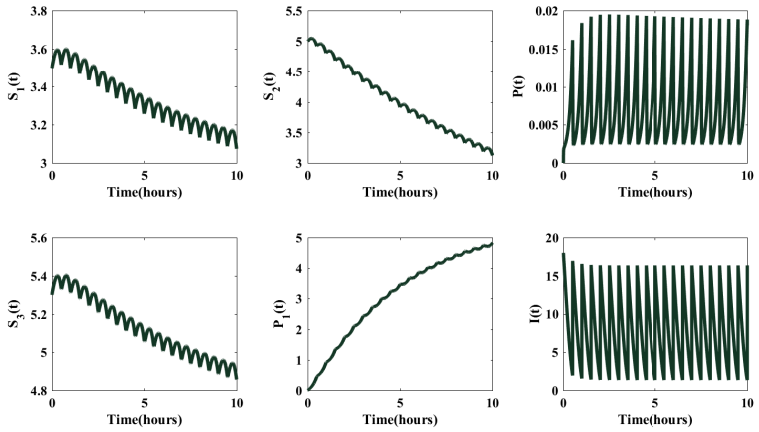

FIGURE 16. Concentration-time curves of the components of model (4) for the impulsive dosing of dual inhibitor of HIV-1 RT/IN with dosing interval $\tau = 5h$. Here, the initial as well as the parameter values and impulse dose I_c are fixed as those in Fig. (14).

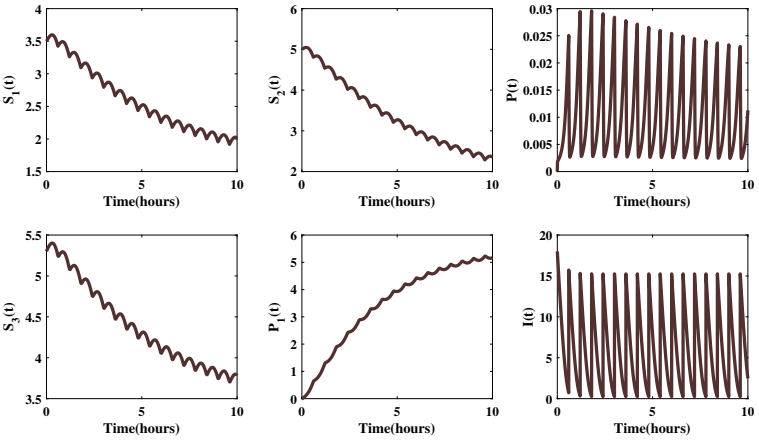

FIGURE 17. Nature of the curves of the components of model (4) for the impulsive dosing of HIV-1 RT/IN dual inhibitor with the period of dosing $\tau = 6h$ using the initial conditions and impulse dose input I_c same as Fig. (14). We have taken the parameter values from Table (1).

well as two different dosing interval to perform the impulse. Curve F and curve F_1 represent the nature change in the concentrations of viral double-stranded DNA (P) and integrated proviral DNA (P_1) respectively in presence of the inhibitor (I) with the impulse dose $20\mu M$ and the time interval of dosing is 8 h, whereas curves

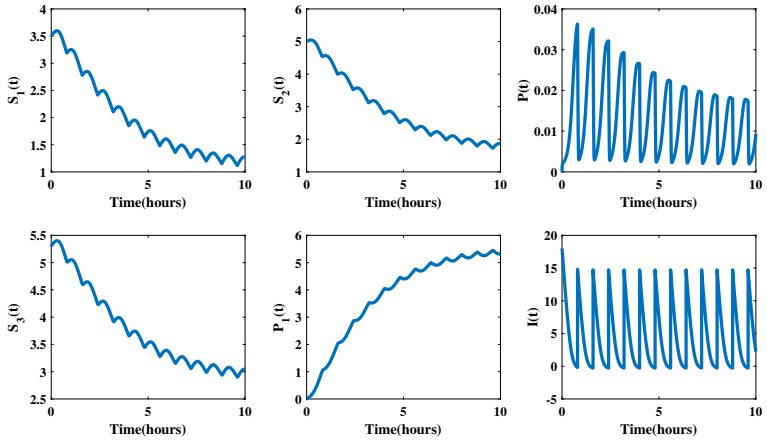

FIGURE 18. Curves of the components of model (4) for the impulsive dosing of dual inhibitor of HIV-1 RT/IN using the same initial values and dose I_c as those in Fig. (14) for the time interval of dosing $\tau = 8h$ and here the parameter values are collected from Table (1).

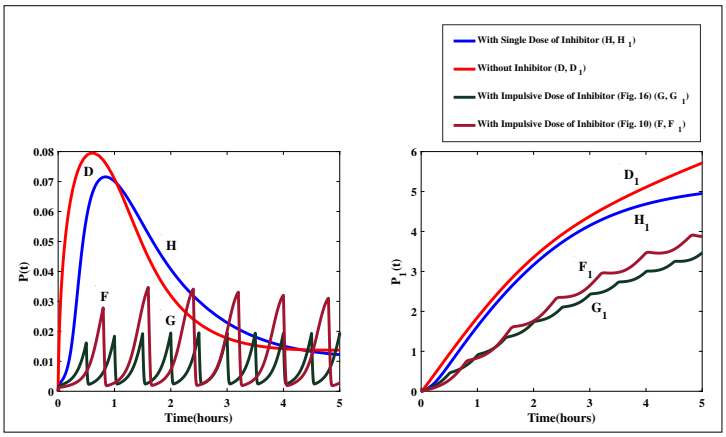

FIGURE 19. Variations of the curves for viral double-stranded DNA concentration and integrated proviral DNA concentration in different situation (without HIV-1 RT/IN dual inhibitor, in presence of HIV-1 RT/IN dual inhibitor with single dose & with multiple doses in impulsive way) are seen in this figure using the initial conditions and parameter values same as the above figures.

G & G_1 illustrate the same thing for the impulse drug dose $15\mu M$ and the dosing interval in this case is 6 h. We can see that the pattern of the curves F & G as well as of the curves F_1 & G_1 are same but the results are better than single dosing

(curves H and H_1). Thus, we can see the significant effect of using dual inhibitor of HIV-1 RT/IN for the treatment of HIV-1 infection.

6. Conclusion

In this paper, we formulated a mathematical model on the HIV-1 reverse transcriptase (RT) and integrase (IN) catalysed reaction for HIV-1 replication and studied the effectiveness of dual inhibitors of HIV-1 reverse transcriptase and integrase which simultaneously work as non-nucleoside reverse transcriptase inhibitor (NNRTI) and integrase inhibitor to combating HIV-1 infection. Although there are several classes of dual inhibitors of HIV-1 RT/IN, here we take bisheteroarylpiperazine compounds (Ex: Delavirdine, Atevirdine) as NNRTI and β-diketo acids (DKAs) group as integrase inhibitor. At first, we analyzed the model introducing dual inhibitor of HIV-1 RT/IN with single dose and then incorporated a one dimensional impulsive differential equation to model the drug dynamics for multiple dose administration. In order to obtain the closed form solution of this impulsive differential equation model, we introduced Lambert W function. Using the Lambert W function, we explicitly expressed the concentration-time curves for multiple dose administration of HIV-1 RT/IN dual inhibitor. In our analytical study, we have established the local stability of the equilibrium point in case of single dose and also expressed the stability of the periodic solution for the case of multiple-dose steady-state and obtained the existence condition ($\frac{I_c}{\tau} < n({K_{i1}}')^n k_3 E_{10} + K_{i2} k_7 E_{20}$) for the periodic solution. We have shown that in order to design a periodic dosing regimen, one large initial dose I^* should be applied followed by a small dose I_c in each dosing interval τ. Our numerical findings also justify the analytical results. Here, in Figs. (9-13), we fix the dosing interval τ to 8h and vary the impulsive dosing amount I_c as well as the initial dose I^*; while in Figs. (14-18), we choose time interval τ as variable and fix the initial dose I^* and impulse dose input I_c to $18\mu M$ and $15\mu M$ respectively. Fig. (9) and Fig. (18) indicate that $5\mu M$ as well as $15\mu M$ dose is not sufficient to suppress the viral load for a large time interval 8h, whereas dosing amount $30\mu M$ and $35\mu M$ may exceed the human body tolerance level for the same dosing period τ and therefore, can cause toxicity, which is identified in Figs. (12-13). Similarly, we observe from Figs. (14-15) that for a shorter dosing interval like 3h or 4h, $15\mu M$ dose can overpower the entire system which is also not safe for a human body. These results imply that for a longer time interval τ, a larger dose is required to maintain a therapeutic effect which is also confirmed in Fig. (8). Moreover, as small as the dose I_c is, the less time is required to approach the steady-state for a given dosing interval τ (Fig. (8)).

The present paper mainly focus on determining the completely analytical solutions for a two-compartment model exhibiting nonlinear Michaelis-Menten elimination kinetics and to provide a basic idea on obtaining an effective dosing regimen for dual inhibitor of HIV-1 RT/IN to treating HIV-1 infection. Therefore, the results obtained in this article can be quite useful for expanding the treatment options to HIV-1 infected patients belonging to the complex HAART therapy.

Acknowledgments

Srijita Mondal was the recipient of "Innovation in Science Pursuit for Inspired Research" (INSPIRE) Program Fellowship, Department of Science and Technology, Government of India.

J.F. Peters was supported by the Natural Sciences & Engineering Research Council of Canada (NSERC) discovery grant 185986, Instituto Nazionale di Alta Matematica (INdAM) Francesco Severi, Gruppo Nazionale per le Strutture Algebriche, Geometriche e Loro Applicazioni grant 9 920160 000362, n.prot U 2016/000036 and Scientific and Technological Research Council of Turkey (TÜBİTAK) Scientific Human Resources Development (BIDEB) under grant no: 2221-1059B211301223.

Appendix A. Appendix. A bit details on dual inhibitors of HIV-1 reverse transcriptase and integrase

A dual action drug is a chemical entity that combines the pharmacophores of two drugs with different mechanisms of action in a single molecule which interacts simultaneously with multiple targets [8]. In recent years, dual inhibitors of HIV-1 reverse transcriptase (RT) and integrase (IN) or Portmanteau Inhibitors have been designed by merging a NNRTI such as 1-[(2-hydroxyethoxy) methyl]-6-(phenylthio) thymine (HEPT) and β-diketo acid derivatives (DKAs) as Integrase Inhibitors [33], [34]. To obtain the merged compound **3**, a DKA moiety was incorporated into the NNRTI **(1)** which is a very potent HIV-1 RT inhibitor, derived from HEPT (Figure (20)) [8]. A second series of substituted merged inhibitors **(4)** were also prepared to enhance the dual activity of these compounds (Figure (20)) [8]. All the merged compounds inhibited both enzymes RT and IN with IC_{50} values in the nano molar (0.0092-0.23 μM) to low micro molar (1.8-7.7 μM) range, respectively and showed very low toxicity when tested in a cell-based assay against HIV-1 replication [8], therefore can be an alternative to combination therapy. In 2008, Wang and Vince [35] reported a new series (Figure (21)) [15] of dual inhibitors of HIV-1 RT and IN by incorporating a diketo acid (DKA) fragment into the NNRTI delavirdine. In 2015, He and Chen group [19] synthesized a series of diarlyprimidine–quinolone analogs (Figure (22)) [15] by hybridizing etravirine (TM125), a second generation NNRTI and elvitegravir (GS-9137), an integrase inhibitor. The marged compounds capable of inhibiting both the enzymes RT and IN provide a new design idea for the development of HIV-1 RT/IN dual inhibitors.

Appendix B. Appendix. Local stability of the periodic solution

Theorem 2. *The periodic solution given by Equation (67) is locally stable.*

Proof. We will show that any solution of model (24) will asymptotically approach the periodic solution (67), for any given initial dose. To do this, we first prove that the solutions given by Equations (59) and (61) are locally stable. Now, solution I_1^* at equilibrium is locally stable if the following condition

$$\frac{\partial(I_1(t_{k+1}^+))}{\partial(I_1(t_k^+))}\Big|_{I_1(t_k^+)=I_1^*} < 1 \tag{70}$$

is satisfied.
Solving the above inequality (70) by applying the chain rule, we have

$$\frac{({K_{i1}}')^n LambertW(Z)}{1+LambertW(Z)}\left[\frac{1}{({K_{i1}}')^n}+\frac{1}{I_1^*}\right] < 1$$

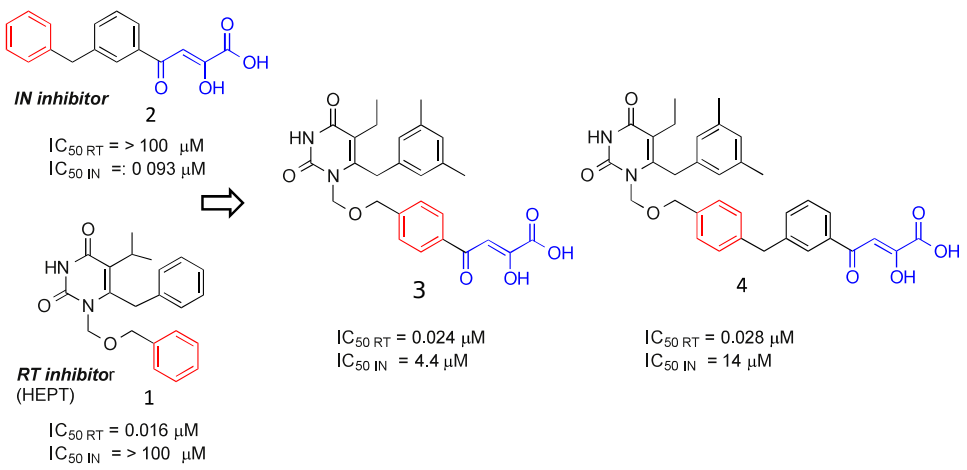

FIGURE 20. Examples of marged dual inhibitors using HEPTs and DKAs as NNRTI and integrase inhibitors.

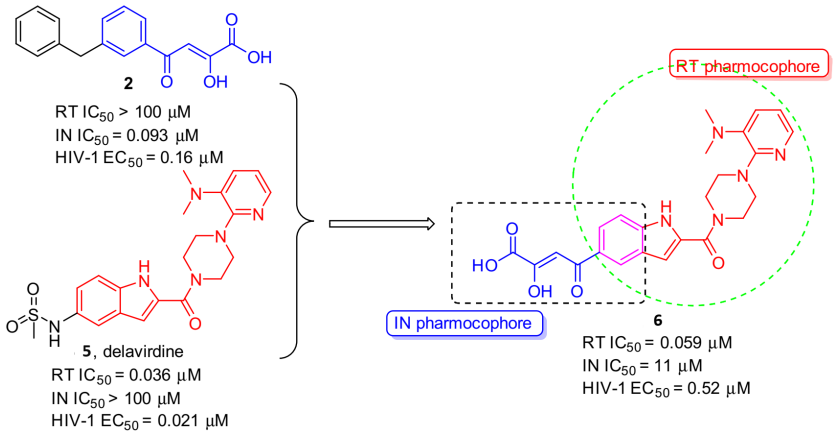

FIGURE 21. Examples of hybrids of Delavirdine and DKAs as dual inhibitors.

i.e.,

$$\frac{LambertW(Z)}{1+LambertW(Z)}\left[\frac{(K_{i1}{}')^n}{I_1^*}+1\right] \quad < \quad 1 \tag{71}$$

where, $Z = \frac{I_1^*}{(K_{i1}{}')^n} exp\left(\frac{I_1^* - n(K_{i1}{}')^n k_3 E_{10}\tau}{(K_{i1}{}')^n}\right)$. Now we show that, if the positive steady-state I_1^* exists then the inequality (71) always holds true. It follows from Equation (54) that we have

$$\begin{aligned} \frac{I_1^*}{(K_{i1}{}')^n} &= LambertW\left(\frac{I_1^*}{(K_{i1}{}')^n} exp\left(\frac{I_1^* - n(K_{i1}{}')^n k_3 E_{10}\tau}{(K_{i1}{}')^n}\right)\right) + \frac{\alpha I_c}{(K_{i1}{}')^n} \\ \frac{I_1^*}{(K_{i1}{}')^n} &= LambertW(Z) + \frac{\alpha I_c}{(K_{i1}{}')^n}. \end{aligned} \tag{72}$$

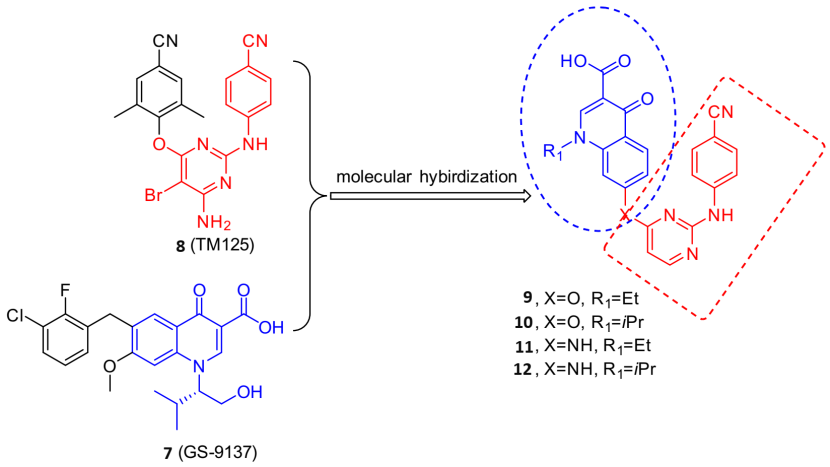

FIGURE 22. Examples of diarlyprimidine–quinolone hybrids as dual inhibitors.

Substituting the above expression for $\frac{I_1^*}{(K_{i1}')^n}$ into (71), we obtain

$$\begin{aligned} & \frac{LambertW(Z)}{1+LambertW(Z)}\left[\frac{1}{LambertW(Z)+\frac{\alpha I_c}{(K_{i1}')^n}}+1\right] < 1 \\ (73) \qquad & \Rightarrow \frac{LambertW(Z)}{(1+LambertW(Z))}\frac{(1+LambertW(Z)+\frac{\alpha I_c}{(K_{i1}')^n})}{(LambertW(Z)+\frac{\alpha I_c}{(K_{i1}')^n})} < 1. \end{aligned}$$

Let us define a function

$$f(x) = \frac{1+LambertW(Z)+x}{LambertW(Z)+x}, x \geqslant 0$$

with $f(0) = \frac{1+LambertW(Z)}{LambertW(Z)}$. This implies

$$(74) \qquad \frac{LambertW(Z)}{1+LambertW(Z)} f(0) = 1.$$

Since

$$\begin{aligned} \frac{d(f(x))}{dx} &= \frac{-1}{(LambertW(Z)+x)^2} \\ &< 0, \end{aligned}$$

we can say that $f(x)$ is a monotonically decreasing function. This implies that the inequality (73) holds true and hence, the local stability of the steady-state I_1^* is proved. Similarly, we can show that the steady-state I_2^* is also locally stable. Now we prove the local stability of the steady-state I^*. Since $I(t) = I_1 + I_2(t)$ (45) and $I^* = I_1^* + I_2^*$ (53), therefore by applying the $\epsilon - \delta$ definition for stability one can prove that I^* is stable, provided both the steady-states I_1^* and I_2^* are stable.

Definition 1. *The equilibrium X_e of an nonlinear autonomous system $X' = f(X)$, $f : D \to \Re^n$ (a locally Lipschitz map from domain $D \subseteq \Re^n$) is*

(*i*) ***stable*** *if for each* $\epsilon > 0$ *there exists a* $\delta(\epsilon) > 0$ *such that*

$$\| X(t_0) - X_e \| \quad < \quad \delta(\epsilon) \Longrightarrow \| X(t) - X_e \| < \epsilon \tag{75}$$

(*ii*) ***asymptotically stable*** *if it is stable and in addition* $\delta(\epsilon)$ *can be chosen such that*

$$\| X(t_0) - X_e \| \quad < \quad \delta(\epsilon) \Longrightarrow \lim_{t \to \infty} \| X(t) - X_e \| = 0. \tag{76}$$

□

References

[1] Dose finding with retroviral vectors: correlation of retroviral vector copy numbers in single cells with gene transfer efficiency in a cell population. Blood **102**(12), 3934–3937 (2003)

[2] Althaus, I.W., Chou, J., Gonzales, A., Deibel, M., Chou, K., Kezdy, F., Romero, D., Aristoff, P., Tarpley, W., Reusser, F.: Steady-state kinetic studies with the non-nucleoside hiv-1 reverse transcriptase inhibitor u-87201e. Journal of Biological Chemistry **268**(9), 6119–6124 (1993)

[3] Anstett, K., Brenner, B., Mesplede, T., Wainberg, M.A.: Hiv drug resistance against strand transfer integrase inhibitors. Retrovirology **14**(1), 1–16 (2017)

[4] Barry, D., Parlange, J.Y., Li, L., Prommer, H., Cunningham, C., Stagnitti, F.: Analytical approximations for real values of the lambert w-function. Mathematics and Computers in Simulation **53**(1-2), 95–103 (2000)

[5] Briggs, G., Haldane, J.: A note on the kinetics of enzyme action. Biochemical journal **19**(2), 338 (1925)

[6] Brussel, A., Sonigo, P.: Evidence for gene expression by unintegrated human immunodeficiency virus type 1 dna species. Journal of virology **78**(20), 11,263–11,271 (2004)

[7] Butler, S.L., Hansen, M.S., Bushman, F.D.: A quantitative assay for hiv dna integration in vivo. Nature medicine **7**(5), 631–634 (2001)

[8] de Castro, S., Camarasa, M.J.: Polypharmacology in hiv inhibition: can a drug with simultaneous action against two relevant targets be an alternative to combination therapy? European journal of medicinal chemistry **150**, 206–227 (2018)

[9] Corless, R., Gonnet, G., Hare, D., Jeffrey, D., Knuth, D.: Advances in comp. Math **5**, 329 (1996)

[10] Craigie, R., Bushman, F.D.: Hiv dna integration. Cold Spring Harbor perspectives in medicine **2**(7), a006,890 (2012)

[11] Das, K., Arnold, E.: Hiv-1 reverse transcriptase and antiviral drug resistance. part 1. Current opinion in virology **3**(2), 111–118 (2013)

[12] Das, K., Arnold, E.: Hiv-1 reverse transcriptase and antiviral drug resistance. part 2. Current opinion in virology **3**(2), 119–128 (2013)

[13] Engelman, A., Mizuuchi, K., Craigie, R.: Hiv-1 dna integration: mechanism of viral dna cleavage and dna strand transfer. Cell **67**(6), 1211–1221 (1991)

[14] Ghosh, P., Peters, J.: Impulsive differential equation model in methanol poisoning detoxification. Journal of Mathematical Chemistry **58**(1), 126–145 (2020)

[15] Gu, S.X., Xue, P., Ju, X.L., Zhu, Y.Y.: Advances in rationally designed dual inhibitors of hiv-1 reverse transcriptase and integrase. Bioorganic & medicinal chemistry **24**(21), 5007–5016 (2016)

[16] Hu, W.S., Hughes, S.H.: Hiv-1 reverse transcription. Cold Spring Harbor perspectives in medicine **2**(10), a006,882 (2012)

[17] Lakshmikantham, V., Bainov, D., Simeonov, P.: Theory of impulsive differential equations. Series in Modern Applied Mathematics, 6. World Scientific Publishing Co., Inc., Teaneck, NJ (1989). xii+273 pp. ISBN: 9971-50-970-9,MR1082551

[18] Li, A., Li, J., Johnson, K.A.: Hiv-1 reverse transcriptase polymerase and rnase h (ribonuclease h) active sites work simultaneously and independently. Journal of Biological Chemistry **291**(51), 26,566–26,585 (2016)

[19] Mao, T.Q., He, Q.Q., Wan, Z.Y., Chen, W.X., Chen, F.E., Tang, G.F., De Clercq, E., Daelemans, D., Pannecouque, C.: Anti-hiv diarylpyrimidine–quinolone hybrids and their mode of action. Bioorganic & medicinal chemistry **23**(13), 3860–3868 (2015)

[20] Mislak, A.C., Frey, K.M., Bollini, M., Jorgensen, W.L., Anderson, K.S.: A mechanistic and structural investigation of modified derivatives of the diaryltriazine class of nnrtis targeting hiv-1 reverse transcriptase. Biochimica et Biophysica Acta (BBA)-General Subjects **1840**(7), 2203–2211 (2014)
[21] Mohammadi, P., Desfarges, S., Bartha, I., Joos, B., Zangger, N., Munoz, M., Günthard, H.F., Beerenwinkel, N., Telenti, A., Ciuffi, A.: 24 hours in the life of hiv-1 in a t cell line. PLoS pathogens **9**(1), e1003,161 (2013)
[22] Murray, J.M., McBride, K., Boesecke, C., Bailey, M., Amin, J., Suzuki, K., Baker, D., Zaunders, J.J., Emery, S., Cooper, D.A., et al.: Integrated hiv dna accumulates prior to treatment while episomal hiv dna records ongoing transmission afterwards. Aids **26**(5), 543–550 (2012)
[23] Rich, D.H.: Evaluation of enzyme inhibitors in drug discovery: A guide for medicinal chemists and pharmacologists. Clinical Chemistry **51**(11), 2219–2220 (2005)
[24] Sarafianos, S.G., Marchand, B., Das, K., Himmel, D.M., Parniak, M.A., Hughes, S.H., Arnold, E.: Structure and function of hiv-1 reverse transcriptase: molecular mechanisms of polymerization and inhibition. Journal of molecular biology **385**(3), 693–713 (2009)
[25] Schauer, G.D., Huber, K.D., Leuba, S.H., Sluis-Cremer, N.: Mechanism of allosteric inhibition of hiv-1 reverse transcriptase revealed by single-molecule and ensemble fluorescence. Nucleic acids research **42**(18), 11,687–11,696 (2014)
[26] Schnell, S., Mendoza, C.: Closed form solution for time-dependent enzyme kinetics. Journal of theoretical Biology **187**(2), 207–212 (1997)
[27] Segel, I.H.: Enzyme kinetics: behavior and analysis of rapid equilibrium and steady state enzyme systems, vol. 115. Wiley New York: (1975)
[28] Shcherbatova, O., Grebennikov, D., Sazonov, I., Meyerhans, A., Bocharov, G.: Modeling of the hiv-1 life cycle in productively infected cells to predict novel therapeutic targets. Pathogens **9**(4), 255 (2020)
[29] Tang, S., Xiao, Y.: One-compartment model with michaelis-menten elimination kinetics and therapeutic window: an analytical approach. Journal of Pharmacokinetics and Pharmacodynamics **34**(6), 807–827 (2007)
[30] Temesgen, Z., Siraj, D.S.: Raltegravir: first in class hiv integrase inhibitor. Therapeutics and clinical risk management **4**(2), 493 (2008)
[31] Usach, I., Melis, V., Peris, J.E.: Non-nucleoside reverse transcriptase inhibitors: a review on pharmacokinetics, pharmacodynamics, safety and tolerability. Journal of the International AIDS Society **16**(1), 18,567 (2013)
[32] Vandegraaff, N., Kumar, R., Burrell, C.J., Li, P.: Kinetics of human immunodeficiency virus type 1 (hiv) dna integration in acutely infected cells as determined using a novel assay for detection of integrated hiv dna. Journal of Virology **75**(22), 11,253–11,260 (2001)
[33] Wang, Z., Bennett, E.M., Wilson, D.J., Salomon, C., Vince, R.: Rationally designed dual inhibitors of hiv reverse transcriptase and integrase. Journal of medicinal chemistry **50**(15), 3416–3419 (2007)
[34] Wang, Z., Tang, J., Salomon, C.E., Dreis, C.D., Vince, R.: Pharmacophore and structure–activity relationships of integrase inhibition within a dual inhibitor scaffold of hiv reverse transcriptase and integrase. Bioorganic & medicinal chemistry **18**(12), 4202–4211 (2010)
[35] Wang, Z., Vince, R.: Design and synthesis of dual inhibitors of hiv reverse transcriptase and integrase: introducing a diketoacid functionality into delavirdine. Bioorganic & medicinal chemistry **16**(7), 3587–3595 (2008)
[36] WHO: Global status report on aids. Tech. rep., WHO (2021). https://www.unaids.org/en
[37] Zarrabi, N., Mancini, E., Tay, J., Shahand, S., Sloot, P.M.: Modeling hiv-1 intracellular replication: two simulation approaches. Procedia Computer Science **1**(1), 555–564 (2010)

Centre for Mathematical Biology and Ecology, Department of Mathematics, Jadavpur University, Kolkata, 700032, India
Email address: mondal.srijita17@gmail.com

Computational Intelligence Laboratory, Department of Electrical & Computer Engineering, University of Manitoba, Winnipeg, MB, R3T 5V6, Canada and Department of Mathematics, Faculty of Arts and Sciences, Adïyaman University, 02040 Adïyaman, Turkey,
Email address: james.peters3@umanitoba.ca

Centre for Mathematical Biology and Ecology, Department of Mathematics, Jadavpur University, Kolkata, 700032, India
Email address: aksarkar@gmail.com

Centre for Mathematical Biology and Ecology, Department of Mathematics, Jadavpur University, Kolkata, 700032, India